



Project: 101095738 – 6G-SHINE-HORIZON-JU-SNS-2022

Project no.:	101095738		
Project full title:	6G SHort range extreme communication IN Entities		
Project Acronym:	6G-SHINE		
Project start date:	01/03/2023	Duration	30 months

D4.1 - PRELIMINARY RESULTS ON THE MANAGEMENT OF RADIO RESOURCES IN SUBNETWORKS IN THE PRESENCE OF LEGITIMATE AND MALICIOUS INTERFERERS

Due date	30/06/2024	Delivery date	30/06/2024
Work package	WP4		
Responsible Author(s)	Saeed Hakimi (AAU)		
Contributor(s)	Gilberto Berardinelli (AAU), Ramoni Adeogun (AAU), Pedro Maia de Sant Ana (BOSCH), Fotis Foukalas (COGN), Christos Tsakos (COGN), Yasser Mestrah (IDE), Renato Barbosa Abreu (Nokia)		
Version	V1.0		
Reviewer(s)	Anders Berggren (SONY), Baldomero Coll Perales (UMH)		
Dissemination level	Public		

VERSION AND AMENDMENT HISTORY

Version	Date (DD/MM/YYYY)	Created/Amended by	Changes
0.1	05/01/2024	Saeed Hakimi	Initial version
0.2	19/02/2024	Saeed Hakimi	<ul style="list-style-type: none"> - Added introduction section with TC tables. - Updated the format and number of figures and tables. - Added the reference section.
0.3	22/04/2024	Saeed Hakimi	<ul style="list-style-type: none"> - Updated the introduction based on initial feedback. - Added a summary and conclusion section.
0.4	05/05/2024	Saeed Hakimi, Gilberto Berardinelli	- Incorporated the latest updates from partners upon preliminary internal review
0.5	31/05/2024	Saeed Hakimi, Gilberto Berardinelli	- Incorporated reviewers' comments by Sony and UMH
0.6	03/06/2024	Saeed Hakimi, Gilberto Berardinelli	- Updated by addressing the reviewers' comments
0.7	26/06/2024	Berit Hvidberg Christensen	Layout check and proofread
0.8	27/06/2024	Saeed Hakimi	Further minor refinements
0.9	27/06/2024	Saeed Hakimi	Last refinements
1.0	30/06/2024	Saeed Hakimi	Final version

Table of Contents

EXECUTIVE SUMMARY	7
1 INTRODUCTION	8
1.1 GENERAL INTRO ON PROPOSED SOLUTIONS	8
1.2 POSITIONING OF THE DESIGNED SOLUTIONS	10
2 RRM FOR IN-X SUBNETWORKS	15
2.1 SUB-BAND ALLOCATION FOR IN-X SUBNETWORKS	15
2.1.1 Centralized approaches for sub-band allocation	15
2.1.1.1 Centralized sub-band allocation solutions using heuristic approaches.....	16
2.1.1.2 Centralized sub-band allocation solutions using AI/ML Approaches	17
2.1.2 Distributed sub-band allocation approach	24
2.1.3 Hybrid sub-band allocation approaches	25
2.1.4 Next Steps	27
2.2 DISTRIBUTED POWER CONTROL FOR IN-X SUBNETWORKS.....	27
2.2.1 Operational Framework of the Distributed MPNN Power Control System.....	28
2.2.1.1 Air-MPNN framework.....	28
2.2.2 Next steps.....	30
3 GOAL ORIENTED RRM.....	31
3.1 PROPOSAL FOR A JOINT NETWORK-CONTROL DESIGN USING REINFORCEMENT LEARNING	31
3.2 NEXT STEPS	34
4 ENABLERS FOR RRM IN SUBNETWORKS.....	35
4.1 SUBNETWORK RESOURCE POOL RESERVATIONS	35
4.2 IBE MITIGATION FOR SUBNETWORK RESOURCES.....	37
4.3 NEXT STEPS	45
5 DETECTION AND MITIGATION OF EXTERNAL INTERFERENCE	46
5.1 TYPES OF ANOMALIES	46
5.2 ANOMALY DETECTION AND CLASSIFICATION METHODS	47
5.2.1 Algorithms and methods used for Anomaly detection.....	48
5.3 IN-X-SUBNETWORKS EXTERNAL INTERFERENCE MITIGATION.....	49
5.3.1 In-X-Subnetworks Cellular and non-cellular interference types	49
5.3.2 Physical mechanisms that lead to non-cellular interference.	50
5.3.3 Non-cellular interference distributions	51
5.3.4 Mismatch decoding Problem	53
5.3.5 Interference mitigation and receiver design	54
5.3.6 Next steps and perspectives	55
6 CONCLUSIONS	57
REFERENCES	58

FIGURES

Figure 1: Reference Deployment for The methods studied in this Deliverable	10
Figure 2: In-factory subnetworks with different rate requirements.....	18
Figure 3: Structure of the proposed DNN model	20
Figure 4: differentiable alternative indicator function and the original indicator function.....	21
Figure 5: Training metrics of DNN.....	23
Figure 6: CDF of the binarization error	23
Figure 7: Rate-conforming InF-Ss	23
Figure 8: Computational runtime for different algorithms	24
Figure 9: Performance evaluation of the different SoTA algorithms	25
Figure 10: Performance evaluation of the different algorithms	27
Figure 11: Distributed power control procedure	30
Figure 12: Air message passing mechanism.....	30
Figure 13: Illustration of the multi-AGV subnetwork joint network-control problem. Each AGV containing a Subnetwork and physically moving to a predefined goal destination.	32
Figure 14: The general framing of the AGV Subnetwork control problem.	33
Figure 15: Overview of the next steps joint network-control design.	34
Figure 16: Example of sub-pool resources reservation based on ePSCCH and sPSCCH.....	37
Figure 17: Example of contiguous and interlaced RB allocation and illustrating potential power leakage.....	38
Figure 18: IBE general component comparison, assuming average EVM of 8%.	38
Figure 19: Example scenario where IBE issues may occur (A) and spectrum power seen from RX UE (B).....	39
Figure 20: Example of IBE scenario in SNE-HC communication (A) and in HC-HC communication (B).....	39
Figure 21: CDF of the average SINR for HC-to-HC.....	41
Figure 22: CDF of the average SINR for SNE-to-HC	42
Figure 23: CDF of the average SINR in high load considering 6 dB reduction for the IBE general term	43
Figure 24: Example of changing transmission starting point for blocking IBE source transmission	44
Figure 25: IBE-aware Inter-UE coordination scheme (Red steps highlight impact on existing IUC procedure).....	45
Figure 26: Point anomaly example in a 2D dataset.....	46
Figure 27: Collective anomaly representation in air temperature records.....	47
Figure 28: Contextual anomalies representation in air temperature records.....	47
Figure 29: An overview of anomaly detection algorithms	49
Figure 30: Coexistence of technologies in the 2.4-GHz band. Measurements made by the National Instruments USRP [33]	51
Figure 31: (Top) Example realizations for each different sub-exponential impulsive noise processes. (Bottom) Optimal decision regions for the different interference processes [34].....	52
Figure 32: Effect of the characteristic exponent parameter α on the α -stable PDF	53
Figure 33: Effect of mismatch decoding, where the linear receiver is used in an impulsive environment.	53
Figure 34: Comparison of the optimal LLR shape with different approximations.	55
Figure 35: Mapping between distribution space and LLR approximation functions space.	56

TABLES

Table 1: Connection of the studied methods with the 6G-SHINE TCs.	11
Table 2: KPIs and KVs targeted by the presented methods.	11
Table 3: Mapping between presented methods and use cases as defined in D2.2	13
Table 4: Standardization potential of the presented methods	13
Table 5: Simulation parameters	22
Table 6: Evaluation parameters used to study the impact of IBE in subnetworks.....	40
Table 8: Parameter description of Stable distribution	52

ABBREVIATIONS

Acronym	Description
AGC	Automatic gain control
AGVs	Autonomous guided vehicles
AP	Access point
CC	Centralized controller
CGC	Centralized graph colouring
CSI	Channel state information
DNN	Deep neural network
ECDF	Empirical cumulative distribution curve
eMBB	Enhanced Mobile Broadband
EN	Entities
FPR	False positive rate
FNN	Fully connected neural network
GCLT	Generalized central limit theorem
HCS	High-capacity elements
HRS	High-rate subnetworks
InF-S	In-factory subnetworks
ISR	Interference-to-signal-ratio
IUC	Inter-UE coordination
IBE	In-band emissions
KPIs	Key performance indicators
KVIs	Key value indicators
LBT	Listen-before-talk
LC	Low capabilities
LRS	Low-rate subnetworks
LLR	Log-likelihood ratio
ML	Machine learning
MDP	Markov decision process

OCB	Occupied bandwidth
PSCCH	Physical sidelink control channel
PSD	Power spectral density
PCA	Principal component analysis
ProSe	Proximity services
QoS	Quality of Service
RA	Random allocation
RCS	Rate conforming subnetworks
RRM	Radio resource management
RSRP	Reference signal received powers
RL	Reinforcement learning
SISA	Sequential Iterative Sub-band Allocation
SINR	Signal-to-Interference-plus-Noise Ratio
SE	Spectral efficiency
SNE	Subnetwork element
SN	Subnetwork
SVM	Support vector machine
TB	Transport block
TRL	Technology readiness level
TPR	True positive rate
URLLC	Ultra-Reliable and Low Latency Communications
UE	User equipment
WNCS	Wireless networked control systems

EXECUTIVE SUMMARY

This deliverable presents an initial description of the radio resource management (RRM) solutions for dense in-X subnetworks studied in 6G-SHINE, including preliminary results. The document explores innovative strategies for sub-band allocation and power control using centralized, distributed, and hybrid methods, aiming at boosting spectral efficiency and maintaining reliable service under stringent Quality of Service (QoS) parameters.

Centralized solutions rely on the presence of a parent network able to receive channel state information from all subnetworks in its coverage areas; while distributed and hybrid solutions refer to the cases where decisions are taken autonomously at the subnetwork only, or partly between subnetworks and parent network, respectively. The adoption of advanced machine learning models –including deep neural networks and message-passing graph neural networks- is highlighted as a promising approach for managing the complexities of dynamic interference, thereby enhancing overall network performance in the emerging 6G ecosystem. In particular, centralized deep neural network approaches for sub-band allocation are shown to improve the amount of subnetwork coping with predefined data rate targets with respect to heuristic solutions while significantly reducing the computational complexity. A combination of centralized sequential iterative sub-band allocation (SISA) and distributed Greedy algorithm is shown to be effective in addressing the case where part of the subnetworks is not able to report their channel state information to the parent network.

A goal-oriented approach to RRM, which integrates control systems' key performance indicators (KPIs) alongside traditional communication metrics, is also discussed. A proposal for joint radio resource management and control design based on reinforcement learning is formulated.

Furthermore, the possibility of using an evolution of the NR side link framework for enabling intra- and inter-subnetwork signaling is extensively studied. An enhancement based on sub-band pool reservation is proposed, and the presence of in-band interference is highlighted as a potential performance-limiting factor to be efficiently counteracted. Promising approaches for dealing with external or uncoordinated interference (e.g., jammers, impulsive noise) relying on autoencoders and detector enhancements are also introduced.

1 INTRODUCTION

This document presents preliminary studies on managing radio resources for in-X subnetworks, focusing on the intricate balance between accommodating legitimate users' needs and combating interference from other legitimate entities or external (including malicious) entities.

Management of radio resources and parameters, such as transmit power, time and frequency resources, precoder, and modulation, is a complex multi-objective optimisation problem further compounded by the unique challenges posed by signal blockage, interference from network densification, and susceptibility to malicious attacks.

A factor ~ 10 densification with respect to 5G is indeed expected in 6G [1]. The inherently dense and mobile nature of subnetwork deployments, such as vehicles in congested traffic or crowded events attended by humans, gives rise to extensive and rapidly fluctuating interference patterns. This dynamic landscape amplifies the complexity of radio resource management far beyond that of traditional wireless setups characterised by static base stations and lower cell densities.

Leveraging the parent network visibility of the operational environment enables more informed decisions regarding radio resource management for each subnetwork. This approach promises more efficient spectrum utilisation but is subject to practical constraints related to communication between subnetworks and the wider network. Challenges include control overhead, quantisation of channel state information, and delays in delivering such information.

While subnetworks may seamlessly integrate into the larger 6G infrastructure and offload the broader network the most demanding services, they must maintain the capability to operate autonomously when connectivity with the broader network is intermittent or absent, particularly in scenarios involving life-critical services (e.g., brake control in vehicles). Some of the subnetworks should possess the capability to sense the available spectrum resources and dynamically select the optimum resources accordingly. In the case of a lack of connection with the broader network, subnetworks should independently determine their optimal radio resources, possibly without the need for explicit signaling between them.

Beyond the realm of legitimate interference, jamming remains a significant concern, especially for life-critical dependent applications. While the physical layer design is intended to bolster resistance against jamming, it must be complemented by methods for detecting and mitigating jamming attacks. It is crucial to differentiate jamming attacks from legitimate interference since response mechanisms can vary.

1.1 GENERAL INTRO ON PROPOSED SOLUTIONS

The solutions presented in this document are a collaborative effort to address the complex challenges inherent in managing radio resources in dense subnetwork scenarios, considering legitimate and external types of interference. Central to the presented approach is the recognition of diverse operational contexts and requirements encountered in real-world deployments. As such, our solutions encompass a spectrum of methodologies ranging from centralized to distributed and hybrid approaches, each tailored to suit specific use cases and environmental conditions.

In the description of the methods, the nomenclature currently being defined in WP2 will be adopted, referring to the relevant subnetwork components. For the work carried out in D4.1, the following elements are relevant:

- **Element with High Capabilities (HC).** An element with high capabilities is a device/node with increased capabilities in terms of networking and computation. Such a node might act as the central communication node in a subnetwork and also might offer compute resources to other devices in the subnetwork. Multiple such HCs can be installed in a single subnetwork. An HC device can be a user equipment as defined by 3GPP or a non-3GPP device.

- Element with Low Capabilities (LC). An element with low capabilities is similar to an HC but has limited capabilities in terms of networking and computation. This can reduce the functionalities that the device provides to the subnetwork. Also, the device might not be connected to the 6G base station. In a hierarchical or nested subnetwork, the LC might act as an aggregator. An LC device can be a user equipment defined by 3GPP or a non-3GPP device.
- Subnetwork Element (SNE). Subnetwork elements are computationally constrained devices that have limited form factor and cost footprint and include devices such as sensors/actuators. A SNE device can be a user equipment as defined by 3GPP or a non-3GPP device.

We refer to deliverable D2.2 for a thorough description of all subnetwork elements [2].

To ensure clarity and coherence, this document is structured to systematically illuminate the key aspects of each proposed solution. It begins by providing an overview of the general context enveloping RRM within subnetworks, thereby laying a foundation for subsequent discussions.

The reference deployment for the topics discussed in this deliverable is depicted in Figure 1, and comprises various technical building blocks. At the centre of this architecture, there is a 6G base station (6G BS), which acts as a parent network and integrates several essential functionalities. Within the 6G BS, diverse elements may exist, including compute nodes primed for RRM computations and components facilitating the offloading of certain functions. Augmenting this architecture are entities (EN) such as robots, production modules, or vehicles, each potentially containing one or more subnetworks (SN). Within these subnetworks, high-capability elements (HCs) serve as central communication nodes. The HCs should have the capabilities to manage the radio resources autonomously in case they are not aided by the parent 6G network.

The deployment scenario dictates the choice of the RRM approach. For subnetworks seamlessly integrated with the umbrella network, centralized RRM methodologies are employed at the 6G BS. Conversely, subnetworks with limited or unreliable connections necessitate the adoption of distributed or hybrid approaches, enabling localised RRM and interference management within one or more entities. Chapter 2 elaborates on this spectrum of solutions, outlining strategies tailored to diverse deployment contexts. This chapter focuses on sub-band allocation and power control as the most effective domains for resource management.

Traditionally, RRM solutions rely on full channel state information (CSI) or other communication-related metrics, optimising network performance. However, in certain application contexts, performance can be optimised not only based on communication metrics but rather on metrics related to the specific application/service (e.g., control cost). Chapter 3 delves into this refined interaction, exploring methodologies that go beyond communication-oriented only solutions to deliver integrated optimal solutions.

Additionally, alongside algorithmic solutions, the empowerment of subnetworks to autonomously tackle interference challenges and RRM necessitates enabling technologies providing the required communication within a subnetwork, as well as for communication among subnetworks and between subnetworks and umbrella networks. Chapter 4 delves into a potential enabler for inter- and intra-subnetwork communication based on the evolution of the NR sidelink framework, including subnetwork resource pool reservation. Mechanisms for reducing the impact of the resulting in-band emissions are discussed.

Beyond the legitimate interference from other ENs, subnetworks may suffer from interferences created by other radio technologies active in the same location (in case they are operating over the same spectrum), and potential malicious interferers (e.g., jammers). While the physical layer is fortified to withstand jamming, the RRM modules must be equipped with robust detection and mitigation strategies. Chapter 5 presents potential solutions for detecting and mitigating such external interferers, using methods such as autoencoders and detector enhancements.

It is imperative to underscore that the concepts and results presented in this document are preliminary. While they offer valuable insights into the efficacy and feasibility of our proposed solutions, they represent only an overview of ongoing research and development efforts. A more comprehensive and elaborate exposition, along with a thorough performance analysis, will be provided in deliverable D4.3, wherein we delve deeper into each solution’s intricacies and empirical findings.

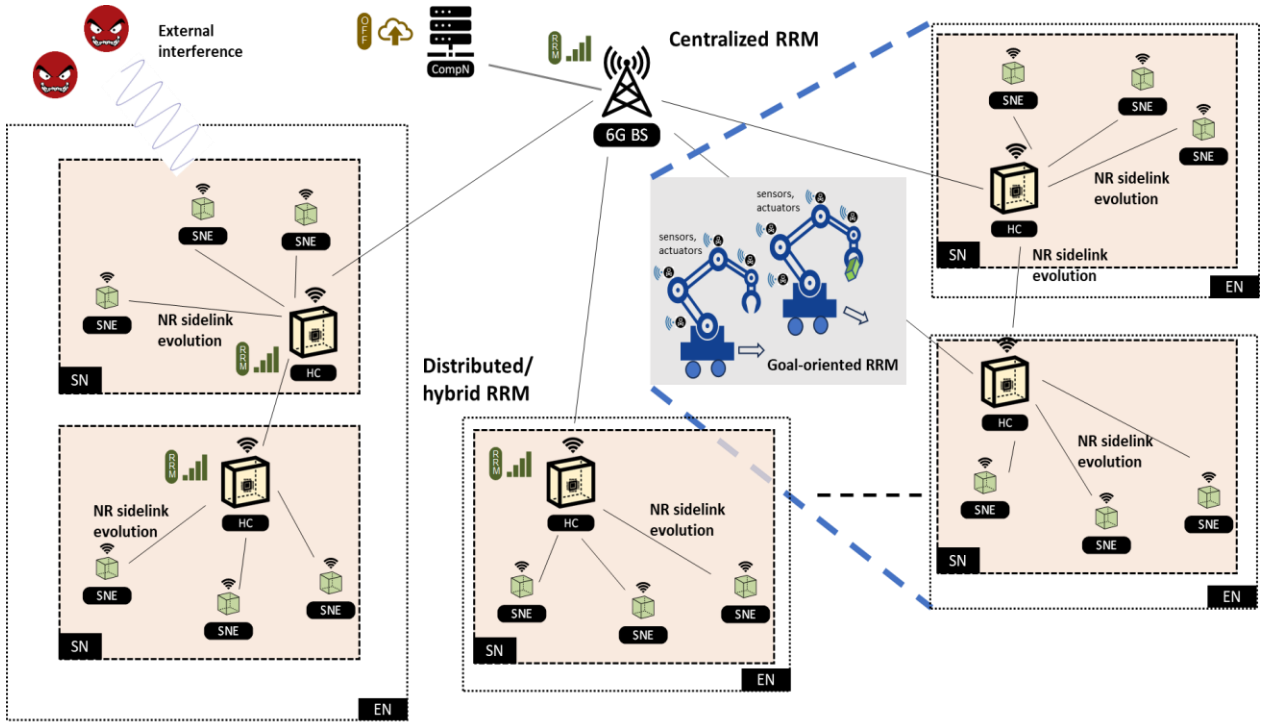


FIGURE 1: REFERENCE DEPLOYMENT FOR THE METHODS STUDIED IN THIS DELIVERABLE.

1.2 POSITIONING OF THE DESIGNED SOLUTIONS

The research presented in this deliverable directly contributes to achieving objective 5 of the project, which is as follows:

Objective 5. Develop cost-effective centralized, distributed or hybrid radio resource management techniques (considering both legitimate and malicious interferers) in hyper-dense dynamic subnetwork deployments.

In the project, 16 technology components (TCs) relevant to in-X subnetworks have been identified. The list of TCs is as follows:

- TC1. In-X data traffic models
- TC2. Channel models for in-X scenarios
- TC3. Sub-THz system model
- TC4. Ultra-short transmissions with extreme reliability
- TC5. Analog/hybrid beamforming/beamfocusing
- TC6. Jamming-aware native PHY design
- TC7. RIS enhancements
- TC8. Intra-subnetwork macro-diversity
- TC9. Flexible/full duplex scheduler
- TC10. Predictive scheduler
- TC11. Latency-aware access in the unlicensed spectrum

- TC12.** Centralized radio resource management
- TC13.** Distributed/hybrid radio resource management.
- TC14.** Jamming detection and mitigation
- TC15.** Hybrid management of traffic, spectrum and computational resources
- TC16.** Coordination of operations among subnetworks in the same entity

The work presented in D4.1 covers TC12-TC14. In Table 1, we present a list of the technology/methods studied in this deliverable and their connection with the original TCs.

TABLE 1: CONNECTION OF THE STUDIED METHODS WITH THE 6G-SHINE TCs.

Technology/method	6G-SHINE TCs
Centralized sub-band allocation solutions using heuristic approaches	TC12
Centralized sub-band allocation solutions using AI/ML approaches	TC12
Distributed sub-band allocation approach	TC13
Hybrid sub-band allocation approaches	TC13
Distributed power control for interference management in in-X subnetworks	TC13
Goal-oriented RRM approaches	TC14
Subnetwork resource pool reservations	TC13
IBE mitigation for subnetwork resources	TC13
Demapper Design for LLR-based decoders to mitigate non-cellular interference.	TC14
Anomaly detection methods for jamming detection and mitigation.	TC14

Table 2 describes the main KPIs and KVis targeted by the presented methods. It is worth mentioning that, since 6G-SHINE is a low technology readiness level (TRL) project, we do not aim at directly measuring the impact of the designed solutions in terms of KVis, as such assessment will only be possible once the designed solutions are implemented and integrated into a coherent system design, which is beyond the scope of the project. Still, KVis are at the centre of our technology design, and we speculate how our solutions can be the basic “bricks” for addressing relevant KVis. A thorough description of how 6G-SHINE research addresses environmental, economic and social sustainability is included in deliverable D2.2 [2]. Given the nature of the research in RRM, the methods presented in D4.1 mainly address environmental and economic sustainability for future in-X subnetwork, though some of the methods can also have beneficial effects on social sustainability.

TABLE 2: KPIs AND KVis TARGETED BY THE PRESENTED METHODS.

Technology/method	Main target KPIs	Targeted KVis
Centralized sub-band allocation solutions using heuristic approaches	Support different minimum spectral efficiency requirements. Communication service availability with a minimum target value of 99.999%.	Improved economic sustainability thanks to more efficient usage of radio resources for industrial communication. Improving quality of experience of consumer use cases thanks to the higher throughput enabled by intelligent resource allocation.
Centralized sub-band allocation solutions using AI/ML approaches		
Distributed sub-band allocation approach		
Hybrid sub-band allocation approaches		

Distributed Power Control for interference management in in-X subnetworks		
Goal-oriented RRM approaches	Path Tracking Error, Linear–Quadratic Regulator (LQR), Throughput and Latency	Economic and social sustainability: by designing a communication system that specifically targets the application goals, we can prevent the overprovisioning of network resources. This not only improves the overall industrial operation but also enhances aspects such as safety and energy efficiency.
Subnetwork resource pool reservations	Low energy consumption and low error probability.	Improved environmental sustainability due to lower energy consumption of the nodes enabled by new subnetwork resource reservation signal which allows SNEs reducing resource pool monitoring effort.
IBE mitigation for subnetwork resources	High data rate and low error probability	Managing IBE issues allows more efficient and reliable communication. This can result in improved economic sustainability and improved environmental sustainability achieved with replacing wired connections by reliable wireless subnetworks.
Demapper Design for LLR-based decoders to mitigate non-cellular interference.	Bit error rate and/or Packet error rate. Throughput Latency. Link Quality Indicator.	Improved economic sustainability, since stronger resilience to external interference can translate to larger production outcome. Social sustainability, since resilience to external interference can translate to improved safety.
Anomaly detection methods for jamming detection and mitigation.	Detection probability False positive rate and/or True positive rate.	

Table 3 presents the mapping of the presented methods to the use case categories (and specific use cases) as defined in deliverable D2.2. We remark that, we do not aim at evaluating each presented method for all the mapped use cases. In our performance evaluation, we rather highlight the main use case or use case category of interest, as we believe the extension to a different use case with similar KPIs is reasonably straightforward.

TABLE 3: MAPPING BETWEEN PRESENTED METHODS AND USE CASES AS DEFINED IN D2.2

Technology/method	Main use case category(ies)	Relevant use cases
Centralized sub-band allocation solutions using heuristic approaches	Industrial, Consumer	Robot control, Unit test cell, Visual inspection cell, Coexistence in factory hall, Immersive education
Centralized sub-band allocation solutions using AI/ML approaches		
Distributed sub-band allocation approach		
Hybrid sub-band allocation approaches		
Distributed Power control for interference management in in-X subnetworks	Industrial	Robot control, Coexistence in factory Hall
Goal-oriented RRM approaches	Industrial	Robot control, Coexistence in factory Hall
Detection and mitigation of external interference	Industrial In-vehicle	Robot control, Wireless zone ECU, Collaborative zone ECU V-3: In-Vehicle subnetwork category
Subnetwork resource pool reservations	Industrial Consumer	Robot control, Unit test cell; Immersive education, interactive gaming
IBE mitigation for subnetwork resources	Industrial Consumer	Robot control, Unit test cell; Immersive education, interactive gaming
Demapper Design for LLR-based decoders to mitigate non-cellular interference.	Industrial In-vehicle	Robot control, Wireless zone ECU, Collaborative zone ECU
Anomaly detection methods for jamming detection and mitigation.	Industrial In-vehicle	Robot control, Wireless zone ECU, Collaborative zone ECU

An outlook of the standardization potential of the proposed methods is presented in Table 4.

TABLE 4: STANDARDIZATION POTENTIAL OF THE PRESENTED METHODS

Technology/method	Standardization potential
Centralized/distributed/hybrid sub-band allocation	These concepts may require specific signaling enhancements, for e.g. measurements report, sub-band allocation indication, to be potentially standardized in 3GPP RAN1
Subnetwork resource pool reservations	This concept has potential relevance in 3GPP RAN1 and RAN2 standardization, for example, in sidelink specifications with enhancements for subnetwork communications.
IBE mitigation for subnetwork resources	These related concepts have potential relevance for 3GPP RAN1 and RAN2 standardization, for example, in sidelink specifications with enhancements for subnetwork communications.
Distributed Power Control for interference management in in-X subnetworks	These concepts may find possible standardization in 3GPP RAN1, for example, in specifications related to downlink power control for interference management as well as synchronization across subnetworks.
Goal-oriented RRM approaches	The related concept may necessitate specific signaling enhancements, which could potentially be addressed by 3GPP RAN2. Additionally, the

	design aspects of joint network-control can be linked to 3GPP RAN3 standardization.
--	---

2 RRM FOR IN-X SUBNETWORKS

This chapter explores RRM in the context of densely deployed In-X subnetworks, which may be either standalone or integrated within a broader 6G network like, e.g. an enterprise network. In response to the increasing need for sophisticated RRM strategies in highly dense and mobile subnetworks, this chapter presents a comprehensive overview of centralized, distributed, and hybrid RRM approaches.

Sub-band allocation and power control are fundamental to Radio Resource Management (RRM), as they determine how efficiently a network uses its frequency spectrum and maintains signal quality while minimising interference and power consumption. These domains are essential for the robust performance and sustainability of high-density networks in the evolving landscape of 6G connectivity. When examining inter-subnetwork communication, two distinct paradigms emerge: one where no explicit inter-subnetwork signaling occurs (potentially relying solely on pilot signals for CSI acquisition) and another where subnetworks engage in explicit message exchanges to fine-tune their operational parameters. In this section, initially, the discussion is focused on sub-band allocation under the assumption of non-communicative subnetworks, later shifting focus to power control scenarios where subnetworks engage in explicit communications with each other.

Centralized strategies are pivotal when subnetworks are seamlessly integrated within a larger network, utilizing a centralized RRM entity at the 6G BS. This approach facilitates comprehensive management of radio resources across all subnetworks, optimizing the allocation process based on complete or near-complete CSI obtained from HCs or LCs. On the other hand, distributed RRM becomes necessary in scenarios where subnetworks operate with intermittent connectivity or need to function autonomously. These solutions empower subnetworks to manage their radio resources independently, dynamically adapting to local conditions without the need for centralized control. This part of the chapter explores algorithms like Greedy selection, which prioritize minimal signaling overhead and adaptability to local interference conditions. Hybrid approaches merge the benefits of centralized and distributed methodologies, offering a flexible strategy that adapts to varying connectivity and CSI availability. These approaches are particularly useful in environments with heterogeneous network capabilities and access levels to the central controller.

Throughout the chapter, a variety of sub-band allocation strategies is examined, from heuristic methods like centralized graph colouring to advanced machine learning techniques that harness the power of deep neural networks for dynamic and efficient resource allocation. Special attention is given to the application of these strategies in practical scenarios, such as factory settings where different subnetworks may have diverse service requirements ranging from Ultra-Reliable and Low Latency Communications (URLLC) to enhanced Mobile Broadband (eMBB). We further contextualize these strategies by considering their application in a simulated factory environment and assessing the performance of various algorithms through comprehensive simulations.

2.1 SUB-BAND ALLOCATION FOR IN-X SUBNETWORKS

2.1.1 CENTRALIZED APPROACHES FOR SUB-BAND ALLOCATION

When in-X subnetworks coexist within the coverage area of a larger 6G network, such as an enterprise network in a factory, centralized RRM becomes feasible. In this section we consider the general deployment as depicted in Figure 1 i.e., there is a centralized RRM entity at the 6G BS which is responsible to manage the radio resources of all the subnetworks. We assume here that the total bandwidth is divided into K equally sized sub-bands, and the 6G BS manages the sub-band to be allocated to each subnetwork. The solutions provided are general and are applicable to a wide range of use cases. For clearer understanding, specific use cases are referenced where appropriate. RRM solutions usually exploits channel state information (CSI) measurements, that could be performed at either HCs, LCs or SNEs. Let us assume that measurements are performed at the HCs. Each subnetwork is assigned orthogonal reference signals in each sub-band; before starting the data transmission stage, the subnetworks transmit their reference signal, assigned by the central RRM entity, using a fixed power. Then,

the HCs measure the reference signal received powers (RSRP) from neighbour HCs on each sub-band. In a centralized solution, the HCs reports the measured RSRPs to the Centralized Controller (CC). Such CC can be co-located with the 6G BS. We denote the RSRP of the i -th LC from the n -th subnetwork on the k -th sub-band as $h_{i,n}^k$. The RSRP matrix of all subnetworks is denoted by $\mathbf{H} \in \mathcal{R}^{K \times N \times N}$.

2.1.1.1 CENTRALIZED SUB-BAND ALLOCATION SOLUTIONS USING HEURISTIC APPROACHES

Various heuristic methods have been proposed in the literature for sub-band allocation, which have demonstrated satisfactory performance.

One well-known centralized approach is **centralized graph colouring** (CGC). In this algorithm, a graph is first defined by considering the sets of vertices ν and edges \mathcal{E} . The vertices represent the subnetworks and edges are added based on the available information. Then, using the completed graph $\mathcal{G}(\nu, \mathcal{E})$, a vertex-coloring algorithm is used to assign a color (equivalent to a sub-band) to each vertex. The vertex-colouring assigns colours in a way so that no neighbouring vertices have the same colour. One way of creating the edges is using the reference signal received powers (RSRP)s received from the subnetworks. For this purpose, the average interference-to-signal-ratio (ISR) of the n -th subnetwork from l -th subnetwork is calculated over the K sub-bands:

$$\overline{W}_n(l) = \frac{1}{K} \sum_{k=1}^K \frac{h_{n,l}^k}{h_{n,n}^k}.$$

After calculating the average ISRs, the n -th vertex will be connected to the $K - 1$ subnetworks with the highest average ISRs. In addition, the averaging could be done locally on the HCs which will decrease the signaling overhead of the CGC algorithm.

Furthermore, the greedy vertex-colouring algorithms try to assign the minimum number of colours to the vertices. To ensure that, the graph is colourable by the available number of colours (corresponding to the number of sub-bands) it adds the edge (i^*, j^*) to the graph as follows,

$$(i^*, j^*) = \arg \max_{\substack{i,j \in \mathcal{N} \\ (i,j) \notin \mathcal{E}}} \overline{W}_l(j),$$

if the number of assigned colours is less than K . Otherwise, it removes the edge, i.e.

$$(i^*, j^*) = \arg \min_{\substack{i,j \in \mathcal{N} \\ (i,j) \notin \mathcal{E}}} \overline{W}_l(j).$$

The process of adding or removing the edges is done sequentially until the number of assigned colours equals the number of sub-bands.

An advanced frequency resource allocation scheme, **known as Sequential Iterative Sub-band Allocation (SISA)** [3], has been designed recently to minimize the sum of ISR across all subnetwork links. The ISR level is calculated based on the RSRP as follows:

$$W_n(l, k) = \frac{h_{n,l}^k}{h_{n,n}^k}, \quad 1 \leq l \leq N.$$

This measurement matrix of size $N \times K$ is calculated at the HC and then forwarded to the CC. After receiving the ISRs from all subnetworks, the controller runs the sequential iterative sub-band allocation algorithm which is described in Algorithm 1. This algorithm starts first with a random allocation that is denoted by the mapping function $\mathcal{C}^0(n), \forall n \in \mathcal{A}$. Moreover, $\mathcal{B}_k^0 = \{n | n \in \mathcal{A}, \mathcal{C}^0(n) = k\}$ denotes the set of active users with the initial allocated sub-band of k . After initialization, the algorithm goes through the active subnetworks sequentially and chooses the sub-band with the lowest mutual ISR according to the current allocation which is described in line 5 of the algorithm. After selecting the sub-band, the allocation is updated at line 6 before moving to the next subnetwork. This process is carried out for M iterations; the allocation vector at the end of the last iteration corresponds to the final allocation. Note that, in the case of mobile subnetworks (or subnetworks experiencing

time-varying channels), the algorithm has to be run frequently enough to cope with the channel variations. Aspects related to mobile subnetworks will be discussed in deliverable D4.3.

Algorithm 1: Sequential Iterative Sub-band Allocation (SISA)

```

Input:  $W_n(l, k)$ ,  $n, l = 1, \dots, N$ ,  $k = 1, \dots, K$ 
1) Initialize:  $C^0(n), \forall n \in \mathcal{A}, \mathcal{B}_k^0 = \{n \mid n \in \mathcal{A}, C^0(n) = k\}$ 
2) for  $m = 1, 2, \dots, M$  do
3)   for  $n = 1, 2, \dots, |A|$  do
4)      $t = |A|(m - 1) + n$ 
5)      $C^t(n) = \arg \min_{1 \leq k \leq K} \sum_{\substack{l \in \mathcal{B}_k^{t-1} \\ l \neq n}} W_n(l, k) + W_l(n, k)$ 
6)      $\mathcal{B}_k^t = \{n \mid n \in \mathcal{A}, C^t(n) = k\}$ 
7)   end for
8) end for

Output:  $\mathcal{B}_k^d$ , where  $d = |A| \times M$ 

```

2.1.1.2 CENTRALIZED SUB-BAND ALLOCATION SOLUTIONS USING AI/ML APPROACHES

While traditional optimization methods and heuristics have proven to be effective in certain scenarios [4], the dynamic and complex nature of in-X subnetworks demands a more adaptive and data-driven approach, necessitating the adoption of advanced artificial intelligence (AI) solutions.

RRM approaches encounter a challenge in their reliance on complete CSI for all desired and interfering links. Acquiring such information in dense deployments can be challenging and time-intensive. A potential solution for centralized power control in subnetworks involves utilizing readily available information instead of full CSI. The power control method proposed in [5] exemplifies this by relying solely on subnetwork positioning information (commonly available at the central controller) and knowledge of the desired link channel gain during the execution phase. However, full CSI is essential during the training phase to compute network performance accurately.

The effectiveness of treating signal processing problems as an unknown nonlinear mapping from input to output and employing deep neural networks to approximate it has been demonstrated in [6]. This approach was applied to approximate interference management algorithms, showcasing its successful application in the realm of signal processing.

In [7], a low complexity centralized transmit power control algorithm is proposed, which is based on the deep unfolding of an iterative projected gradient descent algorithm into layers of a deep neural network. This approach involves learning the step-size parameters. Additionally, an unsupervised learning method is applied for the weights of the Deep Neural Network (DNN), which can be pre-trained online or offline.

The application of graph neural networks has garnered significant attention in addressing the challenges of large-scale interference management. Particularly, this machine learning (ML) paradigm has found utility in power control for In-factory subnetworks (InF-S).

Extending the ML approach to address the sub-band allocation problem, authors in [8] model subnetwork deployment as a conflict graph. An unsupervised learning approach inspired by graph colouring heuristics and the Potts model [9], is proposed to optimize sub-band allocation using graph neural networks.

In-X subnetworks in general and InF-S specially are required to support different services, including URLLC and eMBB, each with distinct requirements. In designing RRM solutions it is necessary to consider these different requirements and try to efficiently utilize the resources to meet the required data rates of various subnetworks.

For better inception let us consider an industrial use case and consider a manufacturing facility comprised of an entity equipped with RRM functionality. This entity harnesses its capabilities to effectively govern radio resources, serving the role of a CC. The factory incorporates numerous short-range cells deployed across robotic systems, production modules, conveyors, and other industrial machinery. Each of these cells, referred to as InF-S, encompasses a central communication node, which functions as the edge processing resource for one or multiple LCs/SNEs within the respective subnetwork. Figure 2 shows a simplified representation of a 2D layout of an InF-S deployment which contains different groups of subnetworks with different required rate or equivalently spectral efficiency (SE). Focus is here on the uplink. The representation shows a single uplink between a LC/SNE and an HC in each subnetwork, and a signaling link from each subnetwork’s HC to a CC. We assume all the LCs/SNEs within a subnetwork are allocated orthogonal resources, i.e. there is no intra-cell interference. Therefore, inter-cell interference is the main limitation to the subnetwork’s SE. For simplicity, for the rest of this section, we assume that each subnetwork serves a single LC/SNE whose transmissions occupy the available bandwidth.

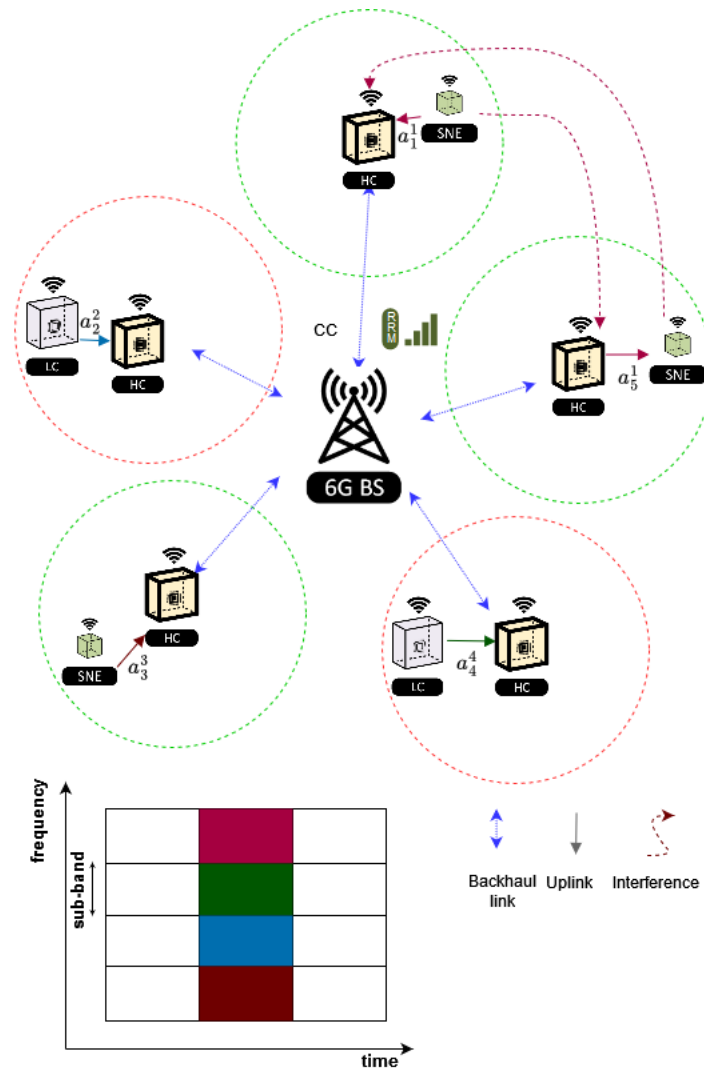


FIGURE 2: IN-FACTORY SUBNETWORKS WITH DIFFERENT RATE REQUIREMENTS

For now, the focus is on the uplink transmission of N subnetworks which are indexed by $n \in \{1, \dots, N\}$. In the considered system, there are K sub-bands, where $k \in \{1, \dots, K\}$ denotes the set of sub-bands which LC/SNE use to transmit data to the HC. It is assumed that each subnetwork has the capability to operate exclusively over a

single sub-band. While eMBB prioritizes high data rates, URLLC services demand low latency and high reliability. The objective of resource allocation is to maximize the number of subnetworks which can achieve to their required rate while ensuring the reliability of critical services. To achieve this goal, the selection of the sub-band, represented by a_n , must be optimized based on current channel conditions. Instead of trying to find the solution of the optimization problem directly through numerical approaches, we transform it into a functional optimization problem. The aim is to find a function that maps the environment (i.e., channel gains) to optimal solutions (i.e., sub-band allocation). To address this functional optimization problem, unsupervised learning techniques are employed.

Leveraging the universal approximation theorem [6], DNNs can approximate a wide range of functions. Therefore, they can be utilized to represent functions that approximate the optimal sub-band allocation strategy for various radio channel conditions.

The achievable SE (bits/s/Hz) at subnetwork n in the k -th sub-band is approximated using the Shannon capacity equation as shown below:

$$SE_n^k = \log_2 \left(1 + \frac{h_{n,n} f_n^k(H) P_m}{\gamma_{m,n}^2 + \sum_{m \in N \setminus \{n\}} h_{m,n} f_m^k(H) P_m} \right),$$

where $h_{m,n}$ represents the channel state of the link from the interfering LC/SNE in subnetwork m , and $f_n^k(\cdot)$ denotes the approximation function for optimal sub-band selection, such that $a_n^k = f_n^k(H)$. The transmit power, denoted as P_m , is uniform across all subnetworks. The term $\gamma_{m,n}^2$ is the receiver noise power calculated as $\gamma_{m,n}^2 = 10^{(-174 + NF + 10 \log_{10}(W_k))}$ where W_k denotes the bandwidth of each sub-band and NF is the receiver noise figure.

The proposed sub-band allocation scheme aims to find the optimal $f_n^k(\cdot)$ to maximize the expected number of subnetworks conforming to the required SE or, equivalently minimize the number of subnetworks that can not reach their target SE or rate. Let SE_n^{req} represent the required SE. The optimal sub-band allocation strategy can be found by solving the following optimization problem:

$$\begin{aligned} \min_{f_n^k \in \{0,1\}} & \sum_{n=1}^N \mathbb{I}(SE_n(f_n^k(\mathbf{H}))) \\ \text{s. t.} & \sum_{k=1}^K f_n^k(H) = 1, \forall n \in \mathbb{N} \end{aligned}$$

where $\mathbb{I}(SE_n)$ is a binary indicator function with a value of 1 if $SE_n \leq SE_n^{\text{req}}$ and 0, otherwise.

The optimization problem involves maximizing the number of rate conforming subnetworks (RCS) subject to a constraint that ensures only one sub-band is used by each subnetwork.

Figure 3 illustrates the configuration of the proposed DNN, which is based on the fully connected neural network (FNN). The DNN takes the channel gain matrix H as input, estimates the function f_n^k , and generates the sub-band allocation vector a_n as the output. In the preprocessing stage, the channel gains undergo reshaping into a one-dimensional vector, a crucial step for integration within the FNN. Subsequently, the values are transformed to the dB scale to restrict the range of possible channel gains. Following this, normalization ensures a zero mean and unit variance. The model then processes the normalized channel gain through the FNN.

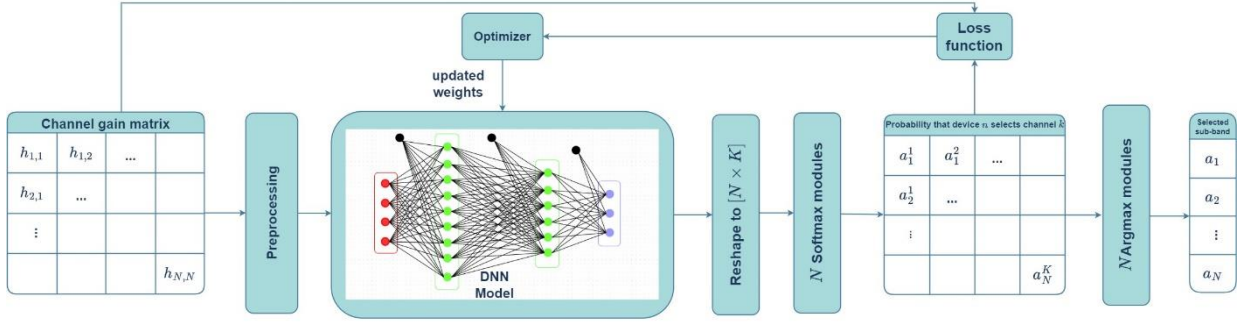


FIGURE 3: STRUCTURE OF THE PROPOSED DNN MODEL

The FNN structure consists of M_L layers, each including a fully connected unit, batch normalization, and a rectified linear unit (ReLU). After the last ReLU, dropout is applied for regularization. The number of hidden nodes for a fully connected unit is set to M_H , with ReLU acting as the activation function. Batch normalization and dropout are employed to mitigate overfitting of the DNN.

The output of the final layer connects to the last fully connected unit, resulting in NK outputs. These outputs are then reshaped into $N \times K$ and fed into N softmax modules. Each softmax module corresponds to the sub-band assignment for a specific subnetwork, executing the softmax operation. This yields K outputs indicating the probability that a sub-band is utilized by the respective subnetwork. The constraint on the sub-band allocation problem is consistently satisfied, as the Softmax outputs sum to one.

As illustrated in Figure 3, the sub-band allocation process differs between training and inference. Specifically, during training, the output of the Softmax module, a_n^k , directly represents the selected sub-band. However, during inference, a_n^k is set to 1 for $k^* = \arg \max_k a_n^k$, and a_n^k is set to 0 for all other k to adhere to the binary constraint in the implementation. This binarization introduces a difference between the resource allocation strategy used in training and that employed during inference, leading to performance degradation. To address the binary constraint, as outlined in the optimization problem, a soft binarization technique is implemented. This technique progressively guides continuous output values towards binary representations during the training steps. Parameterized Softmax modules are leveraged for this purpose, where the n -th softmax layer block's k -th output $\phi_\delta(z_n^k)$ is defined as:

$$\phi_\delta(z_n^k) = \frac{e^{z_n^k/\delta}}{\sum_{k=1}^K e^{z_n^k/\delta}}.$$

Here, z_n^k represents the input to the n -th softmax layer block, and $\delta \in (0,1]$ is a parameter controlling the sharpness of the probability distribution generated by the Softmax. A higher δ value results in a softer, more uniform distribution, while a lower δ value leads to a sharper distribution. For a moderate regime of δ , the parameterized softmax function maintains a non-zero gradient, facilitating efficient training via the stochastic gradient descent algorithm. To mitigate the vanishing gradient problem associated with a small value of δ , an adaptive scaling approach is employed. The scaling factor is decreased at predefined intervals by a reduction factor, ensuring effective training convergence without encountering the vanishing gradient issue.

The decision to adopt unsupervised learning is driven by the significant time investment required to obtain labelled data for supervised training, especially when dealing with a substantial number of subnetworks. Unlike supervised learning, where input data \mathbf{H} is labelled by the output data (optimal sub-band allocation \mathbf{a}_n), our approach leverages unsupervised learning. This allows our DNN to be effectively trained using a carefully designed loss function, eliminating the need for labelled data.

Directly using the objective of optimization problem as the loss function can impact the efficiency of back-propagation-based training. This is due to the non-differentiability of a step function, at specific points. To address this challenge, we employ a modified version of the objective function to ensure differentiability throughout the optimization process. By replacing the binary indicator function with the sigmoid function as a differentiable alternative, the loss function would be:

$$L = \frac{\sigma(SE_n^{req} - SE_n)}{SE_n^{req}},$$

where $\sigma(\cdot)$ denotes the sigmoid function defined as $\sigma(z) = \frac{1}{1 + e^{-z}}$. The denominator is used to weight different required sEs, reflecting practical scenarios where low-rate subnetworks (LRS), such as those involved in robot control applications, are usually critical and should be more reliable. In contrast, high-rate subnetworks (HRS), like those in visual inspection applications, despite high data rate requirement allow for acceptable degradation in instantaneous performance. Figure 4 shows the loss function for HRS and the binary indicator function.

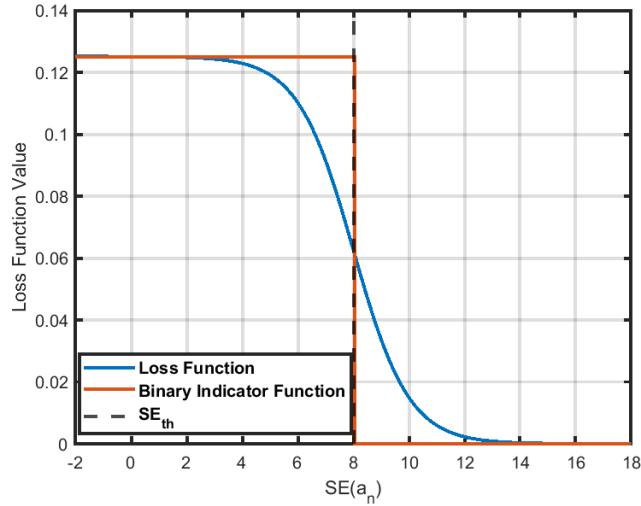


FIGURE 4: DIFFERENTIABLE ALTERNATIVE INDICATOR FUNCTION AND THE ORIGINAL INDICATOR FUNCTION.

In the proposed DNN-aided sub-band allocation, the trained model approximates the sub-band allocation for any channel realization, enabling the scheme's adaptability to various channel conditions without the need for retraining. While the DNN training phase may entail extended computation time, it is conducted offline, i.e., prior to deploying the DNN in the CC. This offline training approach significantly reduces time complexity compared to iterative algorithms.

We consider N InF-S deployed in an $L \times L(m^2)$ factory area. At each InF-S, HC positioned at the center of a circular coverage area with radius R , and a LC/SNE located at a distance d from the HC, ensuring a minimum proximity of d_{min} .

We categorize our subnetworks into two groups: LRS and HRS, which correspond to the robot control and visual inspection use cases, respectively. In Table 20 of deliverable D2.2 [2], the minimum packet size for the robot control use case is specified as 60 bytes, with communication cycles required to be below 100 μ s. This translates to a spectral efficiency (SE) of 0.48 when considering a bandwidth of 10 MHz per sub-band. For the inspection cell use case, the packet size is approximately 100 bytes. Additionally, there is a need to multiplex low latency traffic with high data rate traffic from camera feeds, with approximately 50 Mbps per video camera and 5 Mbps per laser camera. This results in a total data rate of 63 Mbps. Considering a bandwidth of 10 MHz per sub-band, this yields an SE of 6.3. Therefore, we have selected 0.48 and 8 as the values for $SE_{L^{req}}$ and $SE_{H^{req}}$ respectively, such that a certain margin is given for the high-rate subnetworks.

The wireless communication channel model considered for the connection of the LCs/SNEs and HC is based on the model that the 3rd Generation Partnership Project (3GPP) released for InF scenarios. The channel gain in the link between the sensor at subnetwork m and the HC in subnetwork n is expressed as:

$$h_{m,n} = |g_{m,n}|^2 \cdot \Gamma_{m,n} \cdot \Psi_{m,n},$$

where $g_{m,n}$, $\Gamma_{n,m}$ and $\psi_{m,n}$ are complex small-scale fading, path loss and correlated shadowing respectively. The small-scale fading, g , is assumed to be Rayleigh distributed and for the path loss model a dense clutter and low base station height InF (DL) scenario is considered. The specific details regarding the calculation of losses can be found in [10].

Subnetwork links are assumed to have correlated shadowing [11], meaning a source of shadowing will affect several links simultaneously. The first part of the Table 5 shows the simulation parameters for the system model. Note that 20 subnetworks in a 20×20 m area, correspond to a density of 50000 subnetworks/km²; such density is of a factor of $\sim x20$ above typical dense small cells deployments in 5G (~ 2500 base stations/ km²). Regarding the DNN structure, we set the hyperparameters according to the second part of the Table 5.

TABLE 5: SIMULATION PARAMETERS

Parameter	Value
Deployment and System Parameters	
Factory area, $L \times L$	20 m \times 20 m
Number of subnetworks, N	20
Number of sub-bands, K	4
Subnetwork radius, R	1 m
Number of LC/SNE per subnetwork, J	1
Minimum distance between HCs	2 m
LC/SNE to HC minimum distance, d_{min}	0.8
Shadowing standard deviation, λ	7.2 dB
DL clutter density, r , clutter size, d_s	0.6, 2
De-correlation distance, d_c	5 m
Transmit power, P_m	0 dBm
Bandwidth, B	40 MHz
Carrier frequency, f_c	10 GHz
Noise figure, NF	5 dB
LRS required SE, SE_L^{req}	0.4
HRS required SE, SE_H^{req}	8
DNN Parameters	
Number of hidden nodes, M_H	1000
Number of hidden layers, M_L	4
Learning rate, α	$1e^{-5}$
Dropout rate	0.1
Batch size, M_B	1024
Training epochs	200
Training samples	$1e^5$
Validation samples	$1e^4$

The proposed scheme is compared with three baseline schemes: CGC, SISA and Random Allocation (RA). To validate the efficacy of the loss function in handling the binary constraint, the evolution of the loss functions and the binarization error is assessed. The binarization error is defined as $\mathbb{E}[a_n - \text{round}(a_n)]$. Figure 5 illustrates the values of the loss functions for both training and validation data, along with the binarization error and Figure 6 shows the CDF of the binarization error. Considering that optimization variables a_n fall within the range of 0 to 1, the maximum value of the binarization error is 0.5. Post-convergence, the binarization error becomes exceedingly small, confirming that the DNN model proficiently generates binary values.

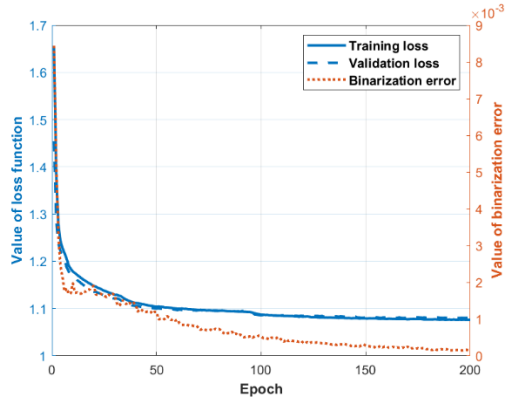


FIGURE 5: TRAINING METRICS OF DNN

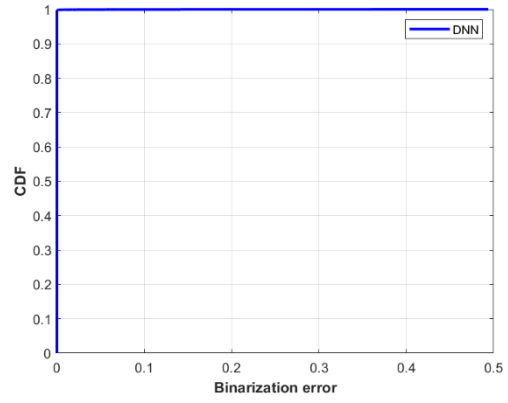
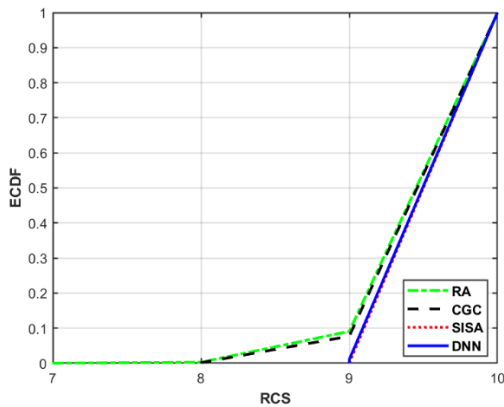


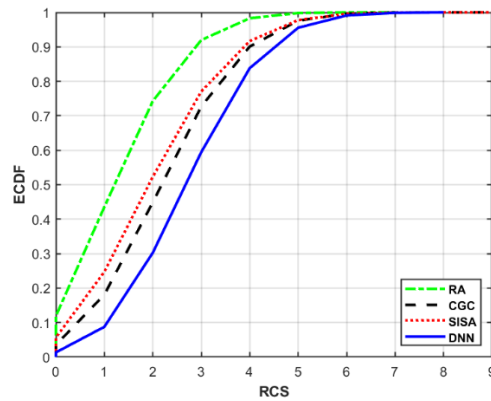
FIGURE 6: CDF OF THE BINARIZATION ERROR

FIGURE 7 PRESENTS THE EMPIRICAL CUMULATIVE DISTRIBUTION CURVE (ECDF) OF THE NUMBER OF RCS FOR TWO DISTINCT SUBNETWORK GROUPS. IN FIGURE 7 (A), IT IS EVIDENT THAT RA AND CGC CANNOT GUARANTEE THE REQUIRED RATES FOR ALL LRS. FOR APPROXIMATELY 10 PERCENT OF THE SUBNETWORKS, THESE METHODS FAIL TO REACH THE SPECIFIED RATE. IN CONTRAST, BOTH SISA AND DNN PERFORM EXCEPTIONALLY WELL FOR LRS. THE MAJORITY OF THE TIME, EMPLOYING EITHER OF THESE ALGORITHMS ENABLES LRS TO MEET THEIR REQUIRED RATES.

Figure 7 (B) illustrates RCS for HRS, showcasing the superiority of the proposed DNN-based sub-band allocation over other benchmarks. On average, three subnetworks of the HRS group can achieve the required rates, while this number is two for SISA. It is important to emphasise that the data traffic of subnetworks may vary at each time interval, necessitating effective data transmission management through a scheduler within the InF-S. In high-load scenarios, where resources are limited, and not all subnetworks can attain their target rates, those falling short of the target may need to adjust their functionality to a lower rate. This adaptation is particularly relevant in use-cases such as vision inspection, where sensors can still operate effectively with lower resolution. Despite the evident advantages of our proposed scheme, it is essential to acknowledge that, in the current landscape of hyper-dense deployment and constrained resources like bandwidth, relying solely on sub-band allocation may not guarantee meeting the expected rate requirements for all subnetworks simultaneously. Therefore, it becomes crucial to consider implementing power control mechanisms or exploring alternative approaches to further enhance the number of subnetworks meeting their rate requirements.



(A): LOW RATE SUBNETWORKS



(B): HIGH RATE SUBNETWORKS

FIGURE 7: RATE-CONFORMING INF-Ss

The trained DNN network consists of simple linear and nonlinear transform units in the forward path, enabling the potential for parallel computation. This design choice facilitates efficient execution and results in low computation time. In contrast, benchmarks like CGC and SISA rely on iterative algorithms, introducing challenges in parallel implementation and limiting their computational efficiency.

The performance evaluations were conducted in a cloud computing environment using resources equipped with an AMD EPYC-Rome Processor (40 cores, 40 threads at 2.9 GHz) and an NVIDIA A40 GPU, with 64GB of RAM. The computational runtime for different algorithms is shown in Figure 8. The significantly lower time required by DNN compared to the benchmarks highlights the efficiency of the DNN-based approach in the context of sub-band allocation, particularly in scenarios involving large-scale computations. For more detailed information on the proposed scheme discussed in this section, readers can refer to [12].

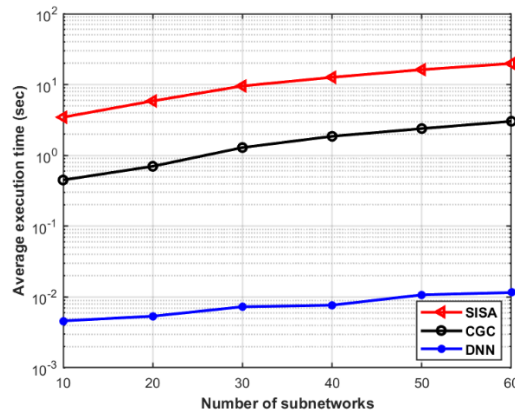


FIGURE 8: COMPUTATIONAL RUNTIME FOR DIFFERENT ALGORITHMS

2.1.2 DISTRIBUTED SUB-BAND ALLOCATION APPROACH

In-X Subnetworks face a dual challenge, which involves autonomous radio resource management to mitigate interference while also being an integral part of a larger network that provides a broader resource optimization perspective. These subnetworks must maintain the capability to function autonomously, especially in scenarios where connectivity with the larger network is intermittent or unavailable, such as those involving critical services for e.g., in-vehicle subnetworks.

In order to be able to operate autonomously, HCs need to possess the capability to sense available spectrum resources and dynamically select the optimal resource accordingly. The goal is to establish implicit distributed coordination schemes, where each subnetwork independently determines its optimal radio resources without relying on explicit communication links between subnetworks.

One of the distributed and simplest algorithms to assign sub-bands to subnetworks is **Greedy selection** where after measuring the aggregated ISR, subnetworks independently select a sub-band as follows:

$$k^* = \arg \min_{k=1,\dots,K} \sum_{l \in \mathcal{A}} \frac{h_{n,l}^k}{h_{n,n}^k}.$$

A comprehensive comparison of SoA solutions in sub-band allocation was conducted through a series of experiments in a simulated factory scenario, identical to the conditions outlined in the initial portion of Table 5. Through these experiments, we evaluated the performance of various algorithms, including SISA, Centralized graph colouring, and Random and Greedy, aiming to elucidate their efficacy in real-world deployment scenarios.

Figure 9 serves as a visual representation of our findings, highlighting the performance characteristics of these algorithms. In Figure 9 (A), we present the CDF of the individual SE for all subnetworks, providing an understanding of the data distribution across different percentile ranges. Meanwhile, Figure 9 (B) illustrates the average SE across all subnetworks, shedding light on the overall performance trends observed.

Our analysis reveals intriguing patterns in algorithm performance. While both SISA and Greedy algorithms exhibit comparable average SE values across all subnetworks, their performance diverges when examined across different percentiles. Specifically, SISA demonstrates a commendable performance for low percentiles, showcasing its ability to maintain fairness in resource allocation among subnetworks. In contrast, the Greedy algorithm excels in high percentile scenarios, indicating its proficiency in optimizing SE under favourable conditions.

These observations have significant implications for practical deployment scenarios, particularly in the context of URLLC use cases. Given its capability for fair resource management, SISA emerges as a preferred choice for applications requiring stringent reliability and latency requirements. However, the Greedy algorithm's prowess in maximizing SE makes it a compelling option in scenarios where high data rates is required.

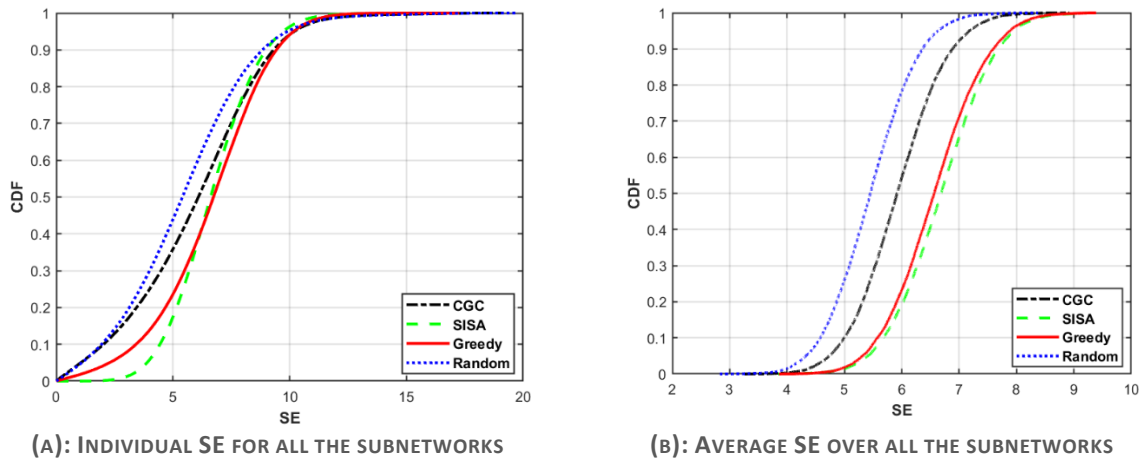


FIGURE 9: PERFORMANCE EVALUATION OF THE DIFFERENT SOTA ALGORITHMS

It is important to highlight the significant advantage of the Greedy algorithm in reducing signaling overhead. This reduction is primarily attributed to the elimination of reference signal transmission, a critical aspect in centralized methods. By removing this step, the Greedy algorithm simplifies the communication process, enhancing efficiency and reducing unnecessary resource consumption. In practical terms, this means that subnetworks employing the Greedy algorithm rely on the local sensed aggregate interference level during the data transmission stage, rather than engaging in additional signaling processes. This streamlined approach not only minimizes overhead but also enhances the scalability and adaptability of the system, particularly in dynamic and complex environments.

Therefore, the Greedy algorithm emerges as a promising solution, offering both performance improvements and operational efficiency in sub-band allocation scenarios. Its ability to mitigate signaling overhead while maintaining effective interference management underscores its relevance in modern communication systems.

2.1.3 HYBRID SUB-BAND ALLOCATION APPROACHES

In certain network scenarios, the availability of CSI and access to a central controller may vary among subnetworks. While some subnetworks possess the capability to measure CSI and communicate with the controller, others operate in disconnected or semi-connected environments, where capability to communicate with the central controller is limited or absent. In such heterogeneous environments, effective resource management becomes a

challenging task, necessitating the exploration of diverse strategies to ensure optimal performance across the network.

One prevalent strategy involves the utilization of partial or outdated CSI by disconnected subnetworks, which may lack direct access to the CC. In this scenario, subnetworks rely on the last policy received from the controller regarding sub-band allocation and power levels. Although this approach may lack optimality due to outdated information or limited context, it offers simplicity and enables decentralized resource management. The CC can leverage this information during resource allocation procedures for connected subnetworks, ensuring a coordinated approach to resource utilization. Alternatively, a hybrid approach combining centralized and distributed methods can be employed to address the challenges posed by disconnected subnetworks. In this approach, connected subnetworks may utilize sophisticated algorithms such as SISA or ML techniques for sub-band allocation, leveraging real-time CSI and controller guidance. Meanwhile, disconnected subnetworks may adopt a Greedy selection strategy based on local observations and historical data. Although disconnected subnetworks may achieve more efficient resource allocation through this hybrid approach, the centralized controller may lack real-time information for RRM in these subnetworks. Consequently, coordination and synchronization mechanisms are crucial to ensure coherence and compatibility between centralized and distributed resource management strategies.

In summary, the management of heterogeneous networks with varying levels of access to CSI and centralized control necessitates the exploration of diverse resource management strategies. By leveraging a combination of centralized and distributed approaches, operators can optimize resource utilization while accommodating the constraints and limitations of disconnected subnetworks. Effective coordination and synchronization mechanisms are vital to ensure seamless operation and performance optimization across the entire network landscape.

In Figure 10, we present a comparative performance analysis of various hybrid sub-band allocation strategies for imperfect CSI against both centralized and distributed algorithms with perfect CSI. The simulation parameters are the same as Table 5 and we suppose 4 of the 20 subnetworks are unable to report their measurements to the CC. The SISA-Greedy approach allows subnetworks connected to the CC to report their measurements and obtain a sub-band assignment based on the SISA algorithm. Meanwhile, subnetworks that are unable to communicate with the CC autonomously choose their sub-band via a Greedy algorithm. Here, the CC lacks any data regarding the non-communicative subnetworks. With the SISA-NN (nearest neighbour) imputation method, while some SNs may not be capable of reporting their measurements, they are still able to receive sub-band assignments. It is assumed that the CC is aware of the locations of all subnetworks, both connected and disconnected ones. For subnetworks that cannot provide data, the CC utilizes the CSI information of the connected nearest neighbour subnetwork to interpolate missing CSI matrix data. In the SISA-Random method, the CC does not recognize the presence of disconnected subnetworks, which independently select their operating sub-band at random. The figure clearly demonstrates that a combination of SISA and Greedy outperforms other hybrid methodologies for incomplete CSI scenarios. Such combination is indeed able to achieve similar performance as centralized SISA in term of individual and average SE, while requiring the least amount of side information from the subnetworks at CC. It is worth to mention however, that there is still a significant gap with SISA at very low percentiles of the individual SE results. Further studies are needed to further enhance the performance for the hybrid framework.

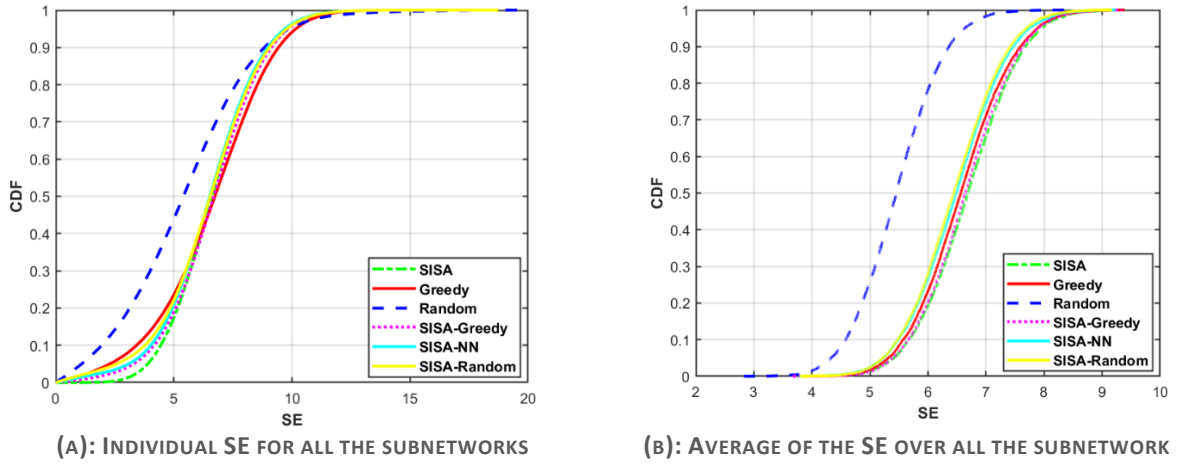


FIGURE 10: PERFORMANCE EVALUATION OF THE DIFFERENT ALGORITHMS

2.1.4 NEXT STEPS

Research presented in Section 2.1 has mainly been on addressing static scenarios, without delving into the complexities of dynamic subnetworks. Moving ahead, the unique challenges and potentials posed by mobile subnetworks are to be tackled. While this deliverable has emphasized the optimization of individual domains, future endeavours will concentrate on the joint optimization of sub-band and power control, potentially yielding more efficient RRM strategies.

In deliverable D4.3, we aim to develop integrated solutions tailored to dynamic subnetworks. The hybrid methods discussed herein are still in their early stages and require extensive research and development to enhance their efficacy. Subsequent work will delve into exploring hybrid solutions that integrate centralized and distributed approaches. These solutions will address diverse types of subnetworks, including those seamlessly integrated within the parent network and those operating autonomously, within a unified framework.

Additionally, results will be benchmarked against the requirements defined in WP2, and the performance targets presented in the proposal..

2.2 DISTRIBUTED POWER CONTROL FOR IN-X SUBNETWORKS

In-X subnetworks are envisioned to be installed in environments where spectrum resources are limited and as a result are designed to operate within the same frequency bands. Previous section has addressed the problem by dividing the available spectrum in multiple sub-bands. Here, we study power control strategies as a solution to manage interference between different subnetworks. Differently from the approaches presented earlier, where signaling happens at most between subnetworks and a central controller, we consider here a distributed scheme where subnetworks are communicating directly with each other for the sake of optimizing transmission power. but subnetworks are still assumed not to be engaged in direct communication with other.

Power control is a challenge widely studied in wireless networks, that fundamentally aims at balancing transmission power to minimize interference while ensuring reliable communication. The drive for more efficient and less computationally intensive power control solutions has led to significant innovations beyond traditional methods like Weighted Minimum Mean Square Error (WMMSE). Machine Learning, especially techniques involving deep learning and neural networks offers a promising alternative particularly in environments where network conditions are constantly changing, such as in in-X subnetworks. Deep Neural Networks (DNNs) have the limitation of not being able to take into consideration network topology, which can limit their effectiveness as the network evolves.

To overcome these limitations recent advancements have focused on Graph Neural Networks (GNNs) which are more suited for data represented graphically like those found in wireless networks. GNNs operate by exploiting

the relationships between nodes(vertices) (which could represent a HC node along with the served SNEs) and edges (representing connections such as interference between different subnetworks) to learn and predict optimal transmission power. This ability of GNNs to utilize the graph structure of wireless networks allows for a more dynamic adaptation process which is more effective in responding to changes in network topology, for instance an addition of another subnetwork. Moreover, the use of Message Passing Neural Networks (MPNNs), a subclass of GNNs, further enhances this capability. While traditional GNNs focus on node-level feature updates, MPNNs introduce a dynamic message passing mechanism which allows nodes to exchange information directly with each other. During this message passing phase of MPNNs, nodes(vertices) exchange messages containing data about their local state and the state of the network, which could include local power levels, channel state information and interference levels. This dynamic information exchange allows for a more responsive and adaptive power control strategy, making MPNNs particularly effective in managing the complex interactions between in-X subnetworks [13].

2.2.1 OPERATIONAL FRAMEWORK OF THE DISTRIBUTED MPNN POWER CONTROL SYSTEM

An HC node should be able to control its downlink power towards the SNEs under a certain distributed power control framework with the goal of limiting interference to neighbour subnetworks. This power control framework could rely on a MPNN between the different subnetworks.. Each HC node along with the served SNEs, of the existing subnetworks, could represent a vertex in a GNN with edges being the channel between different subnetworks. By integrating the MPNN framework, each GNN vertex generates messages which exchanges with the rest of the vertices. These messages contain data about each vertex's current state (vertex feature) as well as information about interference from the neighbour vertices (edge features). The vertices features include the channel coefficients which reflect the direct communication channel used within the subnetwork and obtained through CSI estimation performed by each HC-SNE . Regarding edge features, these include the channel power gain from the interference channels, detailing how much interference a GNN vertex receives from its neighbours. Next, follows an aggregation phase where each GNN vertex aggregates the messages of all neighbours. After aggregating the incoming data each GNN vertex updates its own state and finally makes decisions about its power settings. The above framework depends on accurate CSI for both interference links between vertices (subnetworks) as well as the internal links within subnetworks. To solve the challenges of increased signaling overhead that arise in MPNNs due to the need for CSI estimation and message passing, Air-MPNN has been proposed [14]. Air-MPNN alters the traditional message passing process by introducing an over-the-air aggregation mechanism which significantly reduces the number of transmissions required for each vertex to obtain global information about the network state.

2.2.1.1 AIR-MPNN FRAMEWORK

Contrary to MPNN where CSI and therefore pilot signals are needed for each link, interference or not, Air-MPNN is exploiting the fact that the received power of pilot signals from interference links depends on the channel state of the interference links. Therefore, by directly measuring the accumulated power of the received pilot signals, Air-MPNN captures the aggregated interference without needing individual channel estimation. The Air-MPNN framework enables HC nodes to select the transmit power of the pilot sequence based on vertices features and embeddings during the message passing and aggregation phases. Following this, the HC nodes simultaneously broadcast their pilot signals. The considered Air-MPNN framework only requires all the HC nodes to broadcast the pilot simultaneously for N times, corresponding to N rounds of updates to the GNNs embedding, without additional feedback among the other nodes. After the N rounds of broadcasting pilot signals and processing via message passing and aggregation phases, the Air-MPNN determines the transmit power for data transmission, reducing at the same time signaling overhead.

In the Air-MPNN framework the necessity for updating the graph embedding N times for determining the optimal transmit power for data transmission introduces additional latency. To this end, this could not be applicable for URLLC-like service, where latency and signaling overhead are crucial for some wireless networks. Thus, in [14] it is proposed to update graph embedding once for each transmission frame. This approach builds on the fact that CSI between sequential frames is temporally correlated. An enhanced version of Air-MPNN, named Air-MPRNN, can be implemented which uses information from the previous frame state during graph embedding.

Procedure of Air-MPRNN

Figure 11 depicts the Air-MPRNN framework per frame for distributed power allocation. The problem of the interference management is solved in a distributed manner, meaning that each GNN vertex is a pair of HC-SNE and the messages from neighbouring vertices are represented by the transmit power of pilots and can be aggregated efficiently by evaluating the total interference power. As a result, Air-MPRNN only needs to estimate the total interference power from all the interference links and not from each CSI link independently. Considering that the pilots from the interference links carry the CSI of the interference links, we can treat the aggregation of pilots as the aggregation of the features of the interference links. The basic steps of the Air-MPRNN, which are applied on each frame into a multi-subnetwork environment, can be summarised as follows:

- **Calculation of pilot transmit power:** At the start of each frame, each vertex’s HC generates a message, which is mapped to its pilot signal’s transmit power level. This decision is made by a Multi-Layer-Perceptron (MLP) utilizing the vertex’s previous local state, stored into its embeddings.
- **Simultaneous Pilot Signal Broadcast:** All HCs broadcast their pilot signals simultaneously across the network, referred as the Broadcasting Control Signaling Phase. As a result, a superimposed signal is generated by the summation of all signals. **Error! Reference source not found.** depicts this Air-Message-Passing phase between the subnetworks, where each vertex includes an HC-SNE pair.
- **Aggregation of received signals:** Each vertex’s SNE captures the superimposed signal, which contains the messages from all neighbour vertices. The SNEs, then, feedback the signal back to its HC pair, referred as CSI Control Signaling phase in Figure 11.
- **Local state update (UPD):** Each HC updates its local state, and thus its embeddings, using a MLP that accepts as inputs the previous state and the aggregated messages. This is the embedding update phase in Figure 11.
- **Data transmission power determination:** Finally, with the updated local state, each HC determines the optimal transmission power of the current frame’s data using another MLP. The data subframe phase that follows in Figure 11, is transmitted with the calculated optimal power.

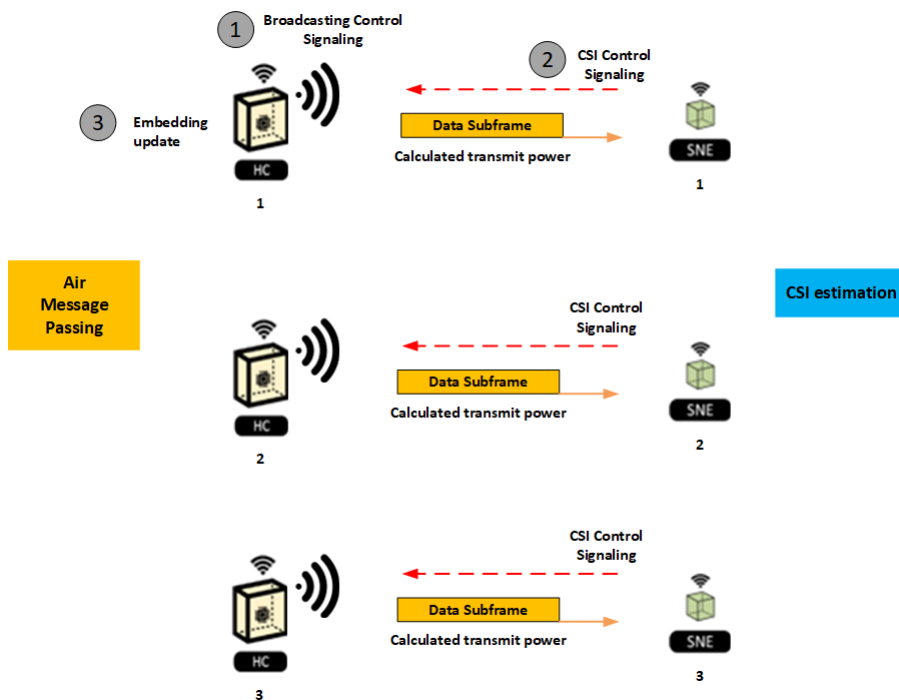


FIGURE 11: DISTRIBUTED POWER CONTROL PROCEDURE

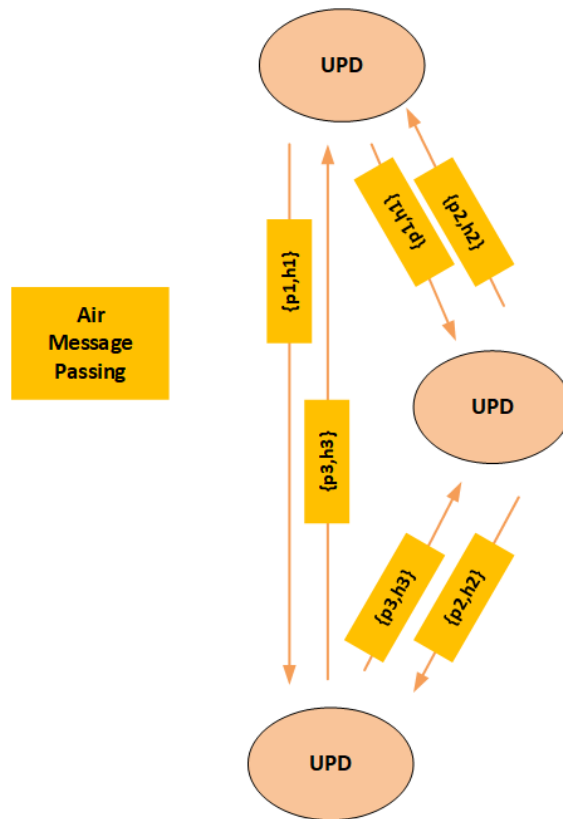


FIGURE 12: AIR MESSAGE PASSING MECHANISM

2.2.2 NEXT STEPS

The above solution is currently under development using the srsRAN open source 5G framework in order to apply the distributed power control using the GNNs in a 3GPP type of system. Special consideration is needed for the downlink power control and overall signaling as depicted in **Error! Reference source not found.** Next steps in this framework include obtaining the results, which will be included in deliverable D4.3. Moreover, the solution with multiple HCs requires synchronization in order to transmit the frame with the power that has been decided in the course of the distributed power control procedure presented above. The way to achieve such synchronization as part of the centralized RRM provided by the parent 6G network is also under study and will be discussed in deliverable D4.3.

3 GOAL ORIENTED RRM

In chapter 2, different approaches for minimising inter-cell interference among multiple dense subnetworks were discussed. The presented solutions focus on optimizing traditional wireless network KPIs, such as meeting minimum rate requirements, rather than optimizing the application itself. This section delves into a goal-oriented approach [15], tackling the problem of mobile subnetworks such as Autonomous Guided Vehicles (AGVs) throughout the factory hall, where two pivotal factors are considered:

- **Contextual Data Utilization:** We leverage context-data, such as velocity and positions, reported from AGVs to the central RRM entity. This data is crucial in managing the interference among the subnetworks.
- **Beyond Resource Management:** Traditional network resource management often yields suboptimal outcomes. Our approach transcends this by focusing on the physical states of the control system. For instance, we control AGV speeds to prevent proximity between co-channel subnetworks, thereby reducing interference. Simultaneously, we ensure the AGVs meet their operational objectives, such as reaching their designated destinations efficiently.

The uniqueness of this problem as a 6G research topic lies in our dual focus. We aim to optimize not just the communication KPIs like Signal-to-Interference-plus-Noise Ratio (SINR), typical in conventional network optimization, but also control KPIs like each AGV's mission time. [15] This holistic view considers the entire factory's performance in the solution, steering us towards an integrated network-control design approach. Such methodologies are pivotal in achieving application-oriented network solutions, balancing both control application performance and network efficiency.

Current literature offers varied solutions focusing either on AGV path planning or network optimization in factory environments. However, these solutions often overlook the dynamic nature of moving subnetworks in the factory, especially considering communication channel factors like multi-path, fast fading, and shadowing. We categorize the existing studies as follows:

1. AGV Control Studies [15][16]: These concentrate on AGV manoeuvring and obstacle avoidance, disregarding the impact of communication on AGV performance.
2. Network Control in AGV Environments [17][18][19]: These works optimize network KPIs for fixed AGV application requirements, potentially leading to network resource overprovisioning.
3. AGV Path Planning with Network Considerations [20][21]: Investigating AGV path planning in static network environments, these studies integrate network KPIs into their analysis.

Additionally, related literature lacks approaches for interference management and resource allocation for subnetworks among AGVs. This gap needs to be addressed as the coexistence of multiple AGVs' subnetworks in proximity poses challenges in terms of interference and resource allocation, as suggested by the industrial use-cases presented in deliverable D2.2 [2].

3.1 PROPOSAL FOR A JOINT NETWORK-CONTROL DESIGN USING REINFORCEMENT LEARNING

Drawing inspiration from prior research in Wireless Networked Control Systems (WNCS) [22][23], we propose a strategy for designing a joint subnetwork-control solution using Reinforcement Learning (RL) principles [24]. WNCS are inherently characterized by uncertainties such as variable network delays, packet losses, and changing system dynamics. RL thrives under such conditions because it learns from interactions with the environment rather than relying on predefined models. By continuously updating its policies based on real-time feedback, RL can adapt to the fluctuating conditions typical of wireless networks, optimizing control actions to improve system performance and stability. This adaptability makes RL an excellent choice for managing and optimizing the performance of WNCS, where traditional control methods might struggle with the network's inherent variability and unpredictability.

We conceptualize the problem as a Markov Decision Process [24], defining a set of states and actions, complemented by a reward function that encapsulates both network and control aspects. Each AGV subnetwork is characterized by a data set encompassing the SINR (I) related to the internal wireless communication within the AGV, the velocity (v), the sub-band allocation (B), and the 2D position coordinates plus the heading angle (x, y, θ), creating a comprehensive state space representation for each AGV : $S_i = \{I_i, v_i, B_i, x_i, y_i, \theta_i\}$.

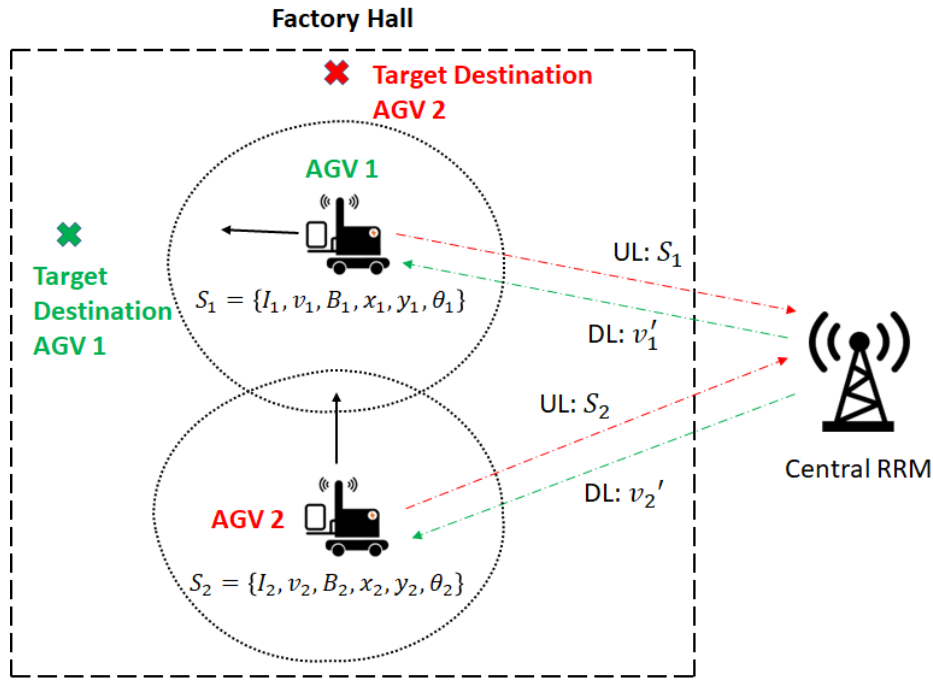


FIGURE 13: ILLUSTRATION OF THE MULTI-AGV SUBNETWORK JOINT NETWORK-CONTROL PROBLEM. EACH AGV CONTAINING A SUBNETWORK AND PHYSICALLY MOVING TO A PREDEFINED GOAL DESTINATION.

As depicted in Figure 13, the AGVs in our system are independently operating with a pre-defined mission: physically move to a goal destination. They routinely send their state information, encompassing key parameters like position, velocity, and sub-band allocation of its in-X wireless subnetwork, to the central RRM unit through an Uplink connection. In response, the RRM dynamically adjusts the speeds of the AGVs, issuing these commands via a Downlink connection. This continuous exchange allows for real-time modulation of AGV behaviour, effectively reducing interference among co-channel subnetworks and enhancing overall network efficiency.

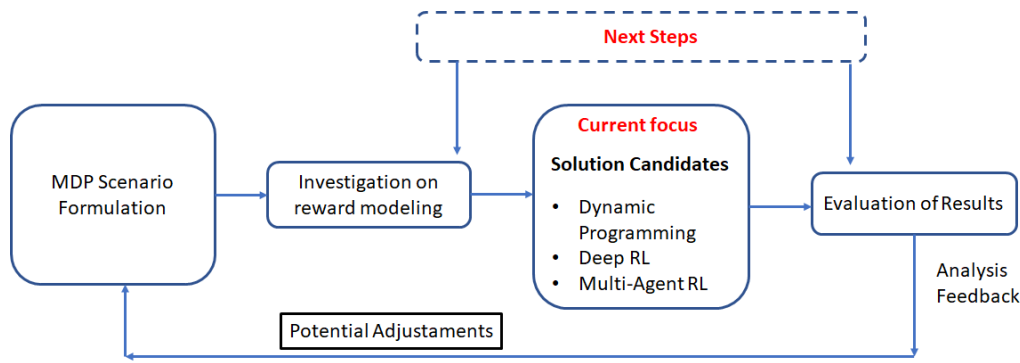


FIGURE 15: OVERVIEW OF THE NEXT STEPS JOINT NETWORK-CONTROL DESIGN.

The exploration of the reward function forms a core component of our investigation. Diverse strategies are to be considered, such as minimizing the mission time of AGVs within a pre-established SINR threshold or defining an upper limit on mission time while simultaneously maximizing the SINR across AGV subnetworks. The overarching objective is to develop an effective AGV coordination policy that maximizes the long-term efficacy of the reward function. As we progress, our research will delve into various solution approaches for this complex problem, employing a spectrum of RL techniques. These include Dynamic Programming, Temporal Difference Learning, advanced Deep Reinforcement Learning, and decentralized RL, specifically multi-agent RL frameworks. This comprehensive approach allows us to adapt and refine our methodologies to suit the intricacies of the problem at hand.

3.2 NEXT STEPS

As we advance our research into optimizing the coordination and management of AGVs in a 6G environment, the contribution to be included in the deliverable D4.3 will focus on further development and refinement of the proposed Reinforcement Learning strategies. We plan to delve deeper into evaluating the efficacy of the RL algorithms through theoretical analysis and controlled simulations, particularly focusing on their performance in dynamic manufacturing settings. These efforts will enhance our understanding of how AGVs interact with each other and the network, with an emphasis on minimizing mission times and enhancing signal quality in complex scenarios. Additionally, we will explore the integration of more granular real-time data, such as environmental variables and AGV operational metrics, to improve the adaptability and accuracy of our RL models. By enriching our models with detailed, dynamic inputs, we aim to develop a robust system capable of predicting and mitigating potential disruptions before they impact the network or AGV performance. The subsequent report will also document the iterative improvements made to our Markov Decision Process models and reward functions. These updates will draw from theoretical insights and simulation results to fine-tune our approach, leading to more sophisticated control strategies.

4 ENABLERS FOR RRM IN SUBNETWORKS

While the previous sections are mainly focused on algorithmic solutions for radio resource management, possible radio enablers implementable in physical (PHY) and medium access control (MAC) layer for supporting the required communication needed in those solutions are presented here.

In a 3GPP context, the support of communication within a subnetwork (e.g. between SNEs and HC device acting as AP) and between subnetwork and 6G parent network can be specified as an evolution of NR Sidelink or should at least be able to coexist with it. This may be justified by the mature Sidelink framework which includes many relevant features for subnetworks, such as, seamless integration with 5G-Advanced and potentially 6G radio access network, operation in-coverage and out-of-coverage, power saving features as Discontinuous Reception (DRX), inter-UE coordination, relaying, support for license and unlicensed bands, among others [25]. Here, we present potential enhancements for enabling subnetwork operations over Sidelink, considering HC to SNE link and HC-to-HC links (e.g., neighbour subnetworks exchanging information).

Technology specification to support direct device-to-device (D2D) communication networks has a development history in 3GPP cellular standards since Rel-12 with the introduction of Proximity Services (ProSe) in LTE, already including in-coverage, out-of-coverage, and partial coverage operation for D2D. The latest 5G NR Sidelink specifications support two resource allocation modes; Mode 1 works as a centralized scheme where gNB schedules the resources to the connected devices for communicating with other devices via Sidelink, and Mode 2 works as a distributed resource allocation for in-coverage and out-of-coverage devices, which autonomously allocate the resources [25].

Despite the advances in Sidelink, still some enhancements are needed for enabling subnetworks with most stringent requirements. The existing Sidelink Mode 2 resource allocation has a flat topology, i.e., there is no distinction of UE roles such as subnetwork HC device or subnetwork SNE device. This means that there is no entity which can be responsible for allocating resources for all the UEs involved in a subnetwork, and each device performs resource selection by itself subject to potential collisions or increased implementation complexity. Also, Mode 2 has challenges in terms of power consumption versus reliability in dense cases, as a continuous/full sensing would be needed by UEs trying to avoid selecting a same resource. In Rel-16 NR Sidelink, resource re-evaluation mechanisms allow a UE to check and reselect if late arriving reservations will cause conflicts with its selected resource, while pre-emption mechanisms allow a UE to re-select if it detects a conflicting high priority reservation. However, these mechanisms require fast reaction and complex implementation for UE that needs to constantly monitor, decide and signal re-selection of resources. In Rel-17, inter-UE coordination (IUC) was introduced in Sidelink for reducing half-duplex issues and hidden-node collisions including two different schemes. In IUC scheme 1, receiver UEs can indicate the (non) preferred resource set indication to transmitter UEs via MAC control messages. In IUC scheme 2, receiver UEs can indicate conflicting resources to transmitter UEs via a feedback channel. The cost of IUC is increased signal overhead and slow reaction since resource conflicts can only be mitigated if reservations are provided well in advance. Additionally, it may be difficult to coexist subnetworks with devices of different characteristics without a static partitioning of the resources. Some issues include in-band emissions (IBE), automatic gain control (AGC) tuning, etc. Here we discuss ways to improve resource coordination by distinguishing control channels for HC-HC and for HC-SNE communications, assuming subnetworks being enabled on top of Sidelink interface. In addition, we discuss issues and enablers for coexistence of multiple HC-SNE communications or HC-HC communications in a shared band.

4.1 SUBNETWORK RESOURCE POOL RESERVATIONS

Existing Sidelink mechanism is not optimized for URLLC since in one hand sensing procedures may be lengthy for better detecting reserved occasions, while on the other hand fast partial sensing and random selection procedures are more prone to collisions. Nevertheless, some Sidelink features, such as the Mode 2 resource reservation and IUC procedures can still be relevant for inter-subnetwork communication and coordination, assuming the critical communication happens within the subnetwork. According to existing Mode 2 mechanism, reservations of future

radio resources can be done in two ways; (i) a semi-persistent transmission manner where the same resources are used for a (longer) period of time and then from time to time subject to re-evaluation, or (ii) an initial transmission (reservation signal) may indicate future resources for repetitions or retransmissions. It should be noted that:

- Reservations are constrained to use the same transport block (TB) size.
- Reservations signal provided in a first transmission is still subject to collisions which may render the entire transmission undecodable.
- Reservations are constrained to a single slot (i.e., a transmission time interval of one TB), hence longer consecutive slots are not feasible for licensed band operation (for unlicensed band, multi-slot reservations are possible in Rel-18) [26].

One enhancement for subnetworks is that HC devices acting as APs should be capable of reserving shares of the Sidelink resource pool for intra-subnetwork communication. Based on this enhancement, the HCs can have the role of selecting resources in the resource pool to be needed for its own purpose or to be used for its subnetwork operation, i.e., communications from, to, and among the SNE devices in the subnetwork.

For enabling such feature, an HC-to-HC control signal can be introduced for subnetworks, e.g. in a form of enhanced Physical Sidelink Control Channel (ePSCCH), to exchange sub-pool reservations. Similarly to existing PSCCH, the ePSCCH indicates its current reservation (e.g., in the first slot where ePSCCH is transmitted) as well as future reservation with sufficient time to resolve conflicts among sub-pool used by different subnetworks, while the conflicts can be resolved by re-evaluation, pre-emption and IUC mechanisms existing in Sidelink. For example, an HC from a neighbour subnetwork may sense the sub-pool reservation indicated by the ePSCCH transmitted by other HCs and exclude all the sub-pool resources from its resource selection procedure.

In addition, the HC may transmit a subnetwork specific PSCCH (sPSCCH) towards its SNEs informing which resources are available. This may be transmitted with a much lower transmit power compared to ePSCCH, and contains resource reservation indications for reception or transmission towards each sub-network device, in the current reserved sub-pool. The SNEs may only need to monitor HC-to-SNE control signal for determining sub-pool resources which can be used for intra-subnetwork communication, by that avoiding inter-subnetwork collisions while reducing sensing overhead for the devices. Figure 16 illustrates an example of a resource pool being used by three subnetworks, which coordinate sub-pool resource usage by means of ePSCCH, used at least for HC-to-HC resource reservation and coordination, and sPSCCH signals towards the SNEs informing which resources are available for intra-subnetwork communication.

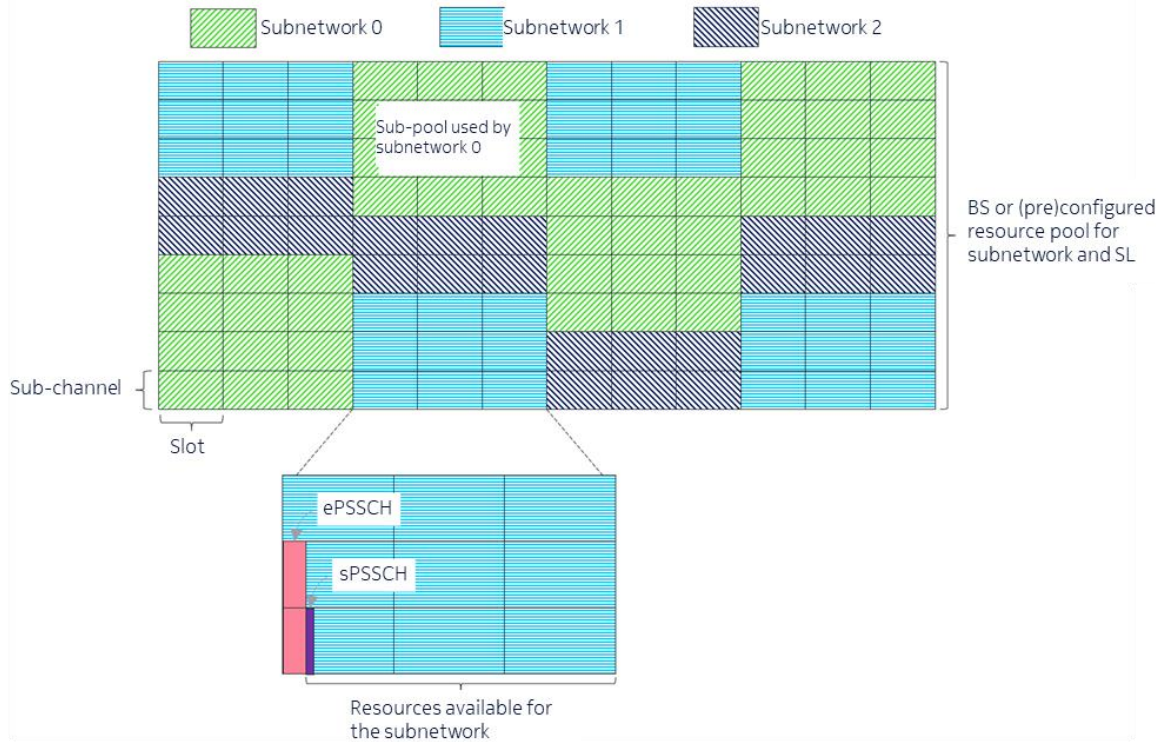


FIGURE 16: EXAMPLE OF SUB-POOL RESOURCES RESERVATION BASED ON ePSSCH AND sPSSCH.

The combination of subnetwork devices and communication between HCs pose a challenge when using the same spectrum, as the two links may need a very different transmit power. For example, an HC may need to transmit with 10-20 dBm to reach another HC (including ePSSCH), while it only needs to transmit between -20 to 0 dBm towards its SNEs (including sPSSCH). This may cause significant adjacent channel leakage if the two transmissions occur in the same time instances and in nearby frequency resources. For that reason, there is a need to ensure that HC-to-HC and intra-subnetwork transmissions are not adjacent in frequency at the same instant, meaning that ePSSCH and sPSSCH may be time multiplexed.

An advantage of the sub-pools reservations is that the SNEs are not required to perform full monitoring of the resource pool, i.e., reducing the effort of detecting and decoding PSSCHs which are not of interest. Further, the DRX active time can be aligned with the sub-pool slots, improving power saving. Additionally, the sub-pool reservations informed from one HC allow its neighbour HCs to perform their own sub-pool reservations such that they avoid as much as possible the adjacent sub-pools that suffer from power leakage, especially if the transmissions from adjacent sub-pools are high power transmissions.

4.2 IBE MITIGATION FOR SUBNETWORK RESOURCES

Another issue which should be considered on the resource management for intra-subnetwork and inter-subnetwork communication is the impact of IBE, especially when assuming frequency domain multiplexing of subnetwork traffic. IBE is the result of power leakage from the allocated transmission resource to the non-allocated transmission resource in the frequency domain, which is mainly caused by transceiver impairments such as IQ imbalance, nonlinearity of RF components, quadrature imbalance and carrier leakage [27]. The IBE is measured as the ratio of the UE output power in a non-allocated resource block (RB) to the UE output power in an allocated RB [28]. The problem is further aggravated in unlicensed bands which the UEs may use interlaced resource allocation, as it was introduced for NR-U and Sidelink unlicensed, for meeting regulatory requirements of occupied bandwidth (OCB) and power spectral density (PSD). An interlace consists of at least 10 resource blocks equally spaced, such

that the OCB requirement is fulfilled (minimum of 80% of the carrier bandwidth according ETSI standards). Figure 17 illustrates an example of interlaced allocation in comparison with a usual contiguous allocation approach.

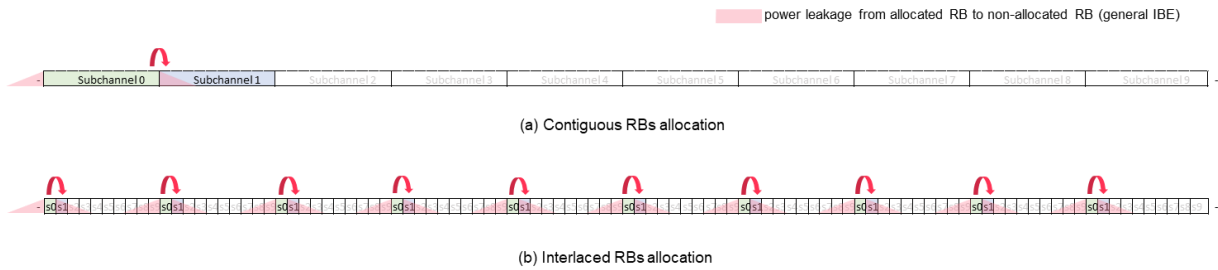


FIGURE 17: EXAMPLE OF CONTIGUOUS AND INTERLACED RB ALLOCATION AND ILLUSTRATING POTENTIAL POWER LEAKAGE.

Figure 18 shows an example of IBE level assuming existing 3GPP requirements, as defined in TS 38.101-1 6.4.2.3 and 6.4F.2.3 for licensed and unlicensed spectrum respectively [28]. Specifically, it shows based on the general limit component of the model, the emission level relative to the average power per allocated RB (assuming allocated 10 RBs) for each non-allocated RB located Δ RBs apart of the allocated RBs. More detailed explanation on the IBE parameters is found on the notes described in the model in the TS 38.101-1 specifications. In this example, for UEs which just strictly satisfy these requirements, the relative emission level towards a neighbour unallocated RB can be up to -24.9 dB in licensed and -10 dB in unlicensed. With interlaced allocation assumed in unlicensed, such high leakage may affect every RB of a neighbour interlace.

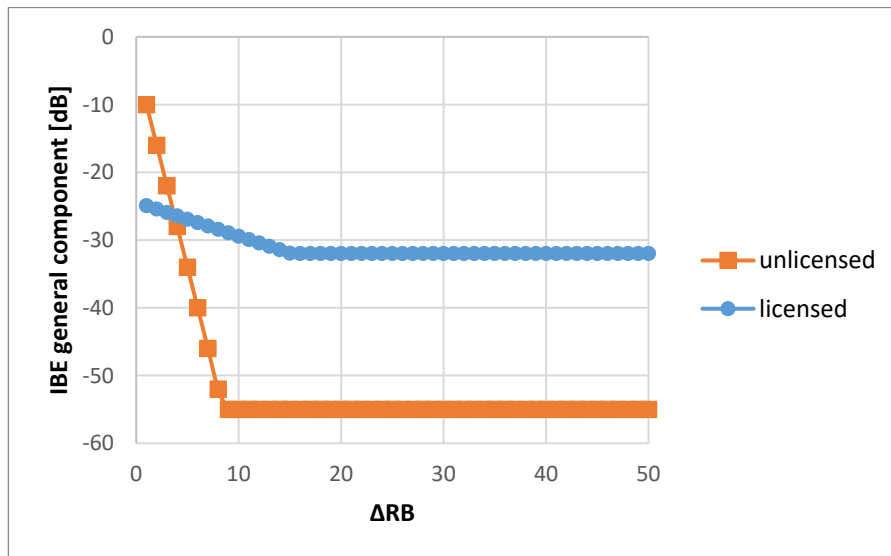


FIGURE 18: IBE GENERAL COMPONENT COMPARISON, ASSUMING AVERAGE EVM OF 8%.

The impact of IBE interference can be significant when two Tx UEs use adjacent resources as well as in resources where the IQ image is located, and where one Tx UE is close to an Rx UE, while the other Tx UE is far from the Rx UE (i.e., near-far problem). In a scenario where devices use distributed resource allocation, a transmitter might not be aware that it is selecting an interlace that will cause an issue for a receiver (e.g. due to the hidden node issue). In Sidelink communication, the hidden (and exposed) node issue is designed to be handled via the IUC framework which was introduced in Rel-17 but has not been designed to handle the IBE aspect.

A simplified scenario where IBE issues occur is illustrated in Figure 19-A. In a subnetwork context, the UEs may be HC devices acting as APs which exchange HC-to-HC data. In another example, a receiver UE (RX UE 1) may be a SNE receiving low power signal from its HC (TX UE 1), while another HC (TX UE 2) may be transmitting data to another

HC (RX UE 2) in an adjacent resource. As illustrated in Figure 19-B, the IBE leakage (red dotted line) from TX UE 1 over the adjacent resource where TX UE 1 transmits will be perceived as increased interference power by RX UE 1, i.e., degrading its SINR for receiving from TX UE 1. Note also that the transmission from TX UE 1 could potentially cause IBE issues to RX UE 2 as well, depending on the transmit power and the channel between these devices.

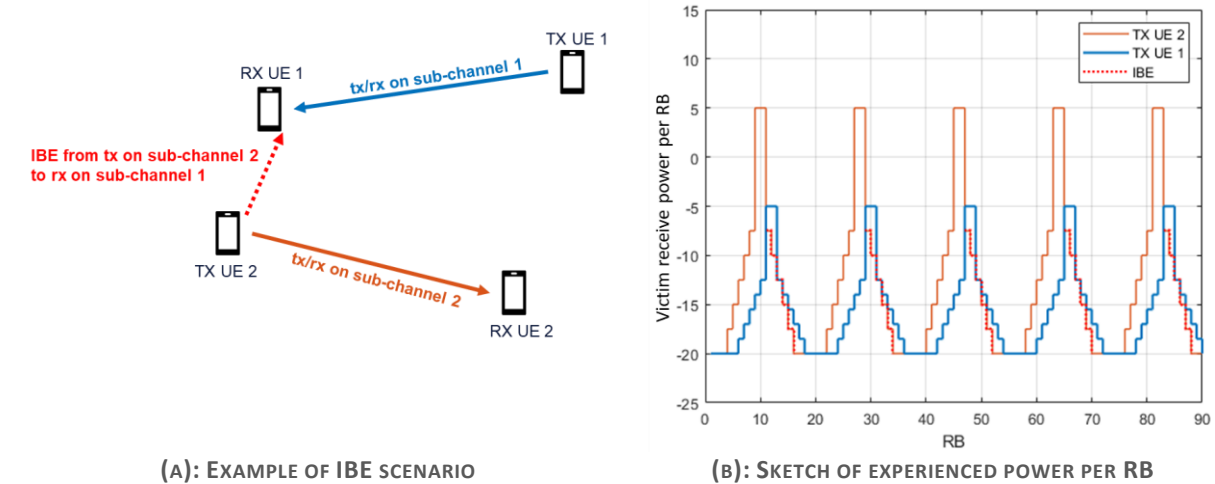


FIGURE 19: EXAMPLE SCENARIO WHERE IBE ISSUES MAY OCCUR (A) AND SPECTRUM POWER SEEN FROM RX UE (B)

The impact of IBE in a subnetwork deployment is evaluated for an indoor classroom scenario, such as for an immersive education use case. The two resource allocation modes are considered, i.e., contiguous and interlaced. Also, the evaluation considers both HC-to-HC communication and SNE-to-HC communication, as illustrated in Figure 20. The HCs may be smartphones which exchange multimedia content to another smartphone located anywhere in the room. These devices are assumed to be of a high-power class transmitting with a power such as 10dBm. While the SNEs are assumed to be of a low-power class and transmit in short distance to their local subnetwork HC with a power of -20 dBm. Such a scenario could be envisioned, for example, for an indoor classroom use case where the SNEs are haptic devices connected to HC devices such as smartphones or smart glasses which allow the pupils to interact in a virtual world.

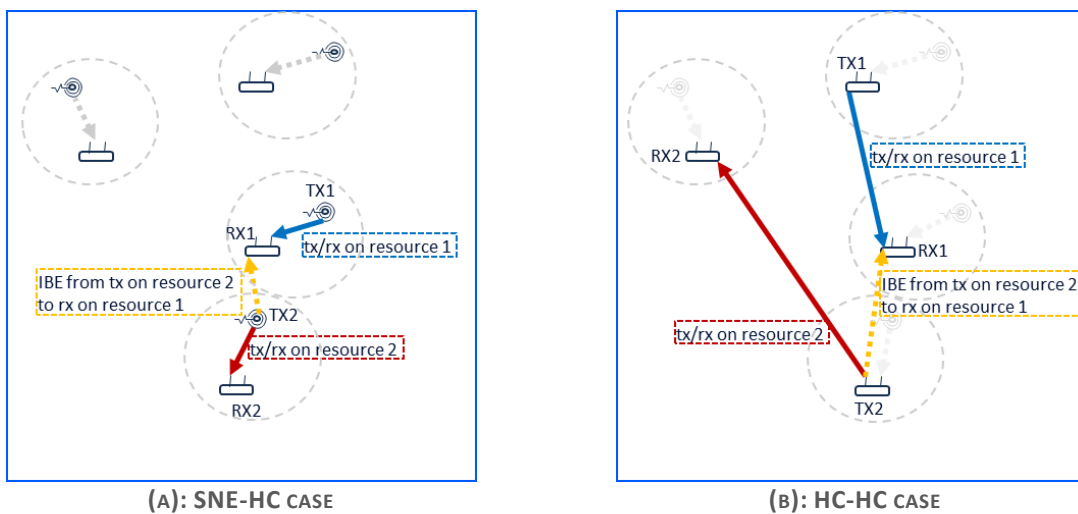


FIGURE 20: EXAMPLE OF IBE SCENARIO IN SNE-HC COMMUNICATION (A) AND IN HC-HC COMMUNICATION (B)

The evaluation is performed using system level simulations with the assumptions mainly based on the evaluation methodology adopted for the 3GPP Rel-18 NR Sidelink evolution [26][29], with some adaptation for the subnetworks use case such as denser deployment in a smaller area and short-distance low-power SNE-to-HC communication. Table 6 summarizes the evaluation assumptions in the study.

TABLE 6. EVALUATION PARAMETERS USED TO STUDY THE IMPACT OF IBE IN SUBNETWORKS.

Parameter	Value
Scenario	A single room of 20 m x 20 m x 3 m (length x width x height) for indoor classroom.
Subnetwork deployment	10 subnetworks are deployed at a random location in the scenario. Each subnetwork consists of 1 HC entity acting as AP and 1 SNE communicating with the HC at a time (frequency multiplexing within subnetwork is not considered) SNEs are deployed with up to 2.5 m distance apart from the HC device which they connect. The subnetworks do not overlap in space.
Channel model	Indoor mixed office (InH) from 38.900.
Traffic modelling	Aperiodic traffic following Poisson arrival model (FTP model 3) <ul style="list-style-type: none"> - 500kB payload (transport layer payload is 1500B) - 0.35 packet/s for the low load (<25% UE buffer occupancy) and 0.75 packet/s for the high load (>55% UE buffer occupancy)
Antenna configuration	1 TX, 2 RX antenna configuration
Carrier frequency and bandwidth	5 GHz carrier frequency with 20 MHz bandwidth (unlicensed band in FR1)
Slot structure	Orthogonal frequency division multiplexing (OFDM) with 15 kHz SCS Assuming Sidelink slot configuration with 14 symbols per slot 10 out of 14 symbols are overhead (to account 2 DMRS, AGC, GP) Control channel equivalent to 2 RBs of the sub-channel
Sub-channel configuration	10 sub-channels of 10 RBs per sub-channel For interlaced allocation it is equivalent to 1 interlace in 20MHz
Scheduling	SL mode 2 autonomous selection randomly in a 20 ms selection window. No inter-subnetwork scheduling coordination
Link adaptation	Fixed modulation and coding scheme (MCS): 256QAM 4/5 for data, QPSK 1/10 for control
Power control	Fixed transmit power of 10dBm for HC in HC-to-HC communication and -20 dBm for SNEs in SNE-to-HC communication
LBT	Listen-before-talk procedure (Type 1 or Type 2 within a channel occupancy time according to TS 37.213) assumed with energy detection threshold of -72 dBm
IBE modelling	Based on minimal requirements from 3GPP TS 38.101-1 [28] <ul style="list-style-type: none"> - Table 6.4.2.3-1 assumed with contiguous RB sub-channel allocation - Table 6.4F.2.3-1 assumed with interlaced RB sub-channel allocation

Note that, by assuming minimal requirements for IBE modelling, the assumptions can be seen as a worst-case scenario since devices could be designed to perform better than these requirements. However, an improved design, e.g. with lower IQ imbalance and lower EVM, implies higher manufacturing cost.

Note also that the frequency of choice in unlicensed band is mainly for the sake of obtaining comparable results for the contiguous versus interlaced allocation which is typically required in unlicensed bands. However, the observations can be generalized for different frequency bands at least for the contiguous allocation cases. First, the results for the HC-to-HC communication are discussed. The empiric cumulative distribution function (CDF) of the average SINR experienced by each receiving node are displayed in Figure 21 for low and high load cases. The solid curves (IBE: no) represent the performance for baseline idealistic cases where IBE effect is not considered, while the dashed curves (IBE: yes) represent the performance when IBE is considered. It can be noticed that there

is a large gap between the ideal case and the cases with IBE. Taking for example the 50%-ile value for interlaced and for contiguous RB sub-channel allocation, respectively, the difference compared to the baseline is 21.5 dB and 11 dB in low load, and 30.8 dB and 19.6 dB in high load. The performance is noticeably worse for the interlaced allocation given that the worst-case IBE general term affects not only a few RBs but all the RBs of the adjacent sub-channel, and moreover in a higher level (see Figure 18) as compared to the general term of contiguous allocations.

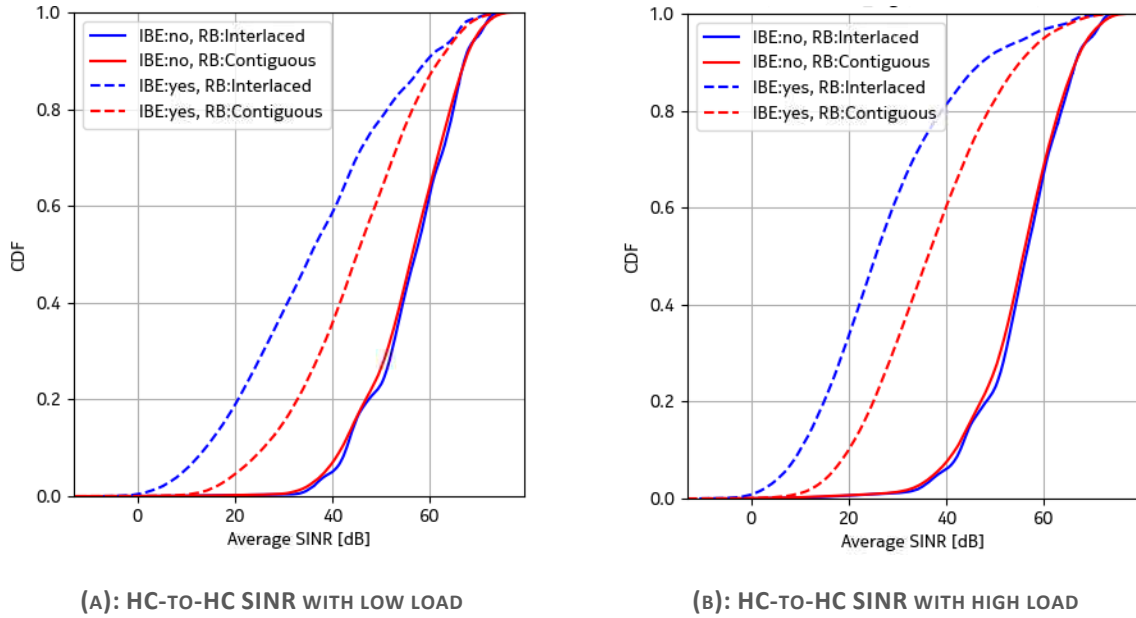


FIGURE 21: CDF OF THE AVERAGE SINR FOR HC-TO-HC

Figure 22 shows the average SINR performance for the SNE-to-HC communication cases. It is noticeable that the performance gap between the ideal case without IBE and the cases when IBE is considered is much lower compared to the HC-to-HC communication. For the 50%-ile, the differences are 6.1 dB and 2.5 dB in low load, and 10.6 dB and 4.2 dB in high load, for interlaced and contiguous RB sub-channel allocation, respectively. The IBE impact for SNE-to-HC is lower compared to HC-to-HC because the latter uses higher power, and in addition it is more susceptible to near-far effect, given that HCs may communicate with any HC in a room, and not only to their vicinity. Still, the effect for SNE-to-HC is not negligible even in low load, specifically in the low percentiles of the distribution.

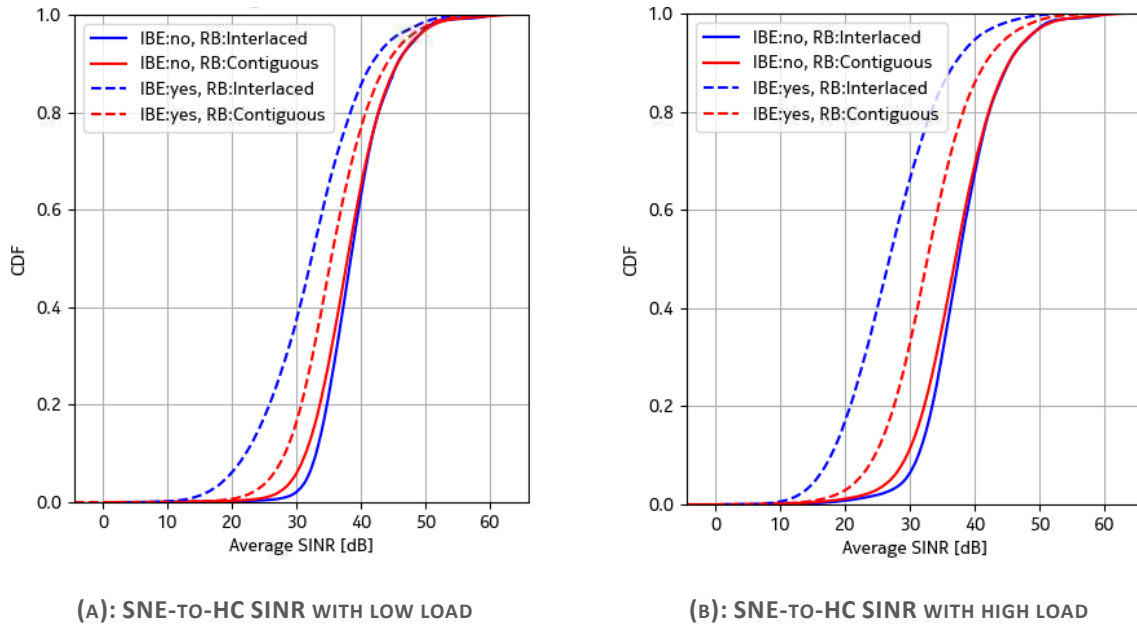


FIGURE 22: CDF OF THE AVERAGE SINR FOR SNE-TO-HC

Based on the above, it is observed that IBE should be considered if frequency-domain multiplexing is applied for subnetwork communications including HC-to-HC and SNE-to-HC in a shared carrier. For interlaced allocation, the impact is significant on the average SINR performance when load increases. On the lower percentiles of SINR CDF, which dictates URLLC performance, the impact is still high even in low load with interlaced or contiguous allocation modes.

Below we discuss some potential enablers to mitigate the IBE issue for subnetworks includes the following:

- **Enabler A: Time-domain multiplexing**

Time-domain multiplexing of communication between subnetworks and within subnetworks can be applied to avoid IBE issue at least when the QoS requirements allow. In terms of complexity for RRM implementation, TDM is a low complex alternative which should provide performance close to the baseline, i.e., with no IBE shown in the results. However, the latency performance may be degraded with TDM, due to the TX slot alignment depending on the frame configuration. For completely mitigating the issue with TDM, for example, by assigning dedicated slots for each subnetwork in a band, the average latency may increase linearly with the number of subnetworks, which may be prohibitive for low latency use cases.

- **Enabler B: Stricter IBE requirements in UE radio transmission and reception standards**

In this study it was assumed that the HC devices and SNEs implementation just meet the exact minimum requirements for in-band emission as specified in 3GPP TS 38.101-1. However, if subnetwork devices implementation can perform better than the current minimum requirements, the impact of IBE can be much reduced. Figure 23 shows an example of performance for high load case when the IBE general term is assumed to be 6dB lower than the current limit in the specifications. For the HC-to-HC case, the difference on the 50%-ile SINR compared to the baseline reduces to 17.8 dB and 12.6 dB for interlaced and contiguous allocation, respectively. For the SNE-to-HC case, the difference reduces to 3.2 dB and 1.7 dB. The advantage of this solution is that it reduces the need for a RRM mechanism to deal with the issue, therefore avoiding higher complexity in the resource selection procedure in the device. However, stricter RF requirements in standards, may impose more advanced physical layer designs, such as better isolation and filtering to reduce spurious emissions, therefore impacting hardware costs. That may be acceptable for HC devices, however, for low cost SNEs such solution may not be desirable.

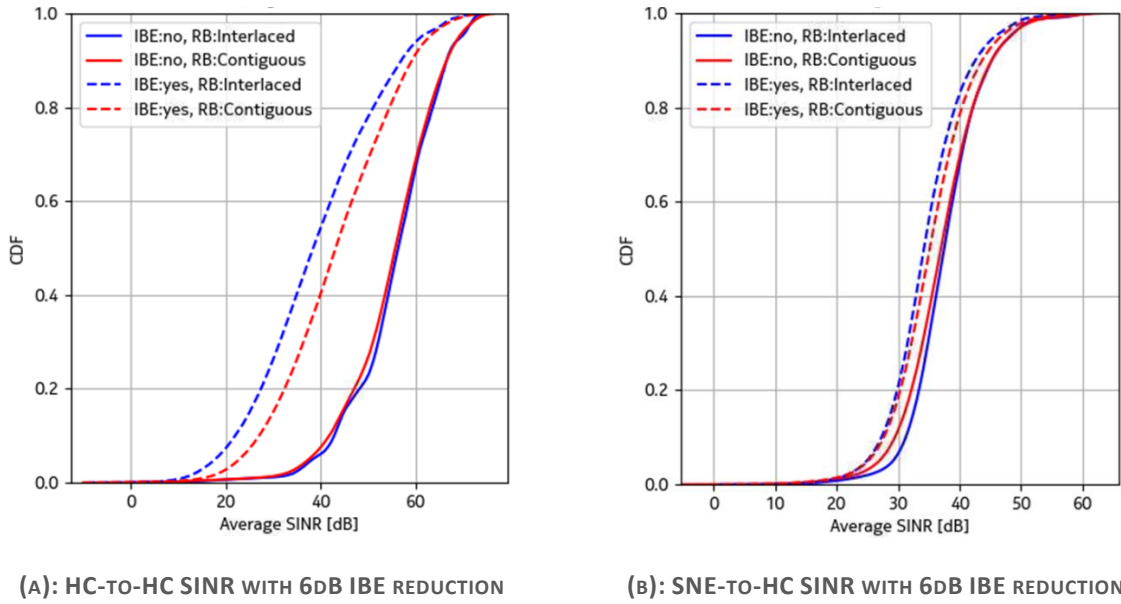


FIGURE 23: CDF OF THE AVERAGE SINR IN HIGH LOAD CONSIDERING 6 DB REDUCTION FOR THE IBE GENERAL TERM

- Enabler C: Adapting transmission starting point for blocking adjacent resource transmissions in vicinity

At least for unlicensed spectrum operations, where listen-before-talk procedures are implemented, a subnetwork device may be configured to apply a change on its transmission starting point when determining that a resource reservation from another subnetwork device (detected, for example, via sensing procedure in sidelink) indicating a transmission on the same slot and band (albeit with a different interlace) will (i) cause IBE issues to the reception of the subnetwork devices own transmission or (ii) that the subnetwork devices own transmission will cause IBE issues to the reception of other subnetwork device transmission. This solution can be implemented using cyclic prefix (CP) extensions available in the Rel-18 Sidelink evolution.

In one example illustrated in Figure 24-B, a UE A which is preparing to transmit on a selected resource on an interlace a , if it senses a resource reservation from a UE B on an interlace b and the separation in frequency w between the interlaces is within at least one interval $W=[wL, wH]$, UE A may change its transmission starting point to be later than the starting point of the transmission of UE B. The change of transmission starting point may be decided based on one or more of the following criteria:

- Resource reservation of UE B is for a transmission with higher priority than of UE A.
- Resource reservation of UE B has an estimated receive power y higher than Y .
- Distance d between UE A and the receiver of UE B is lower than a value D , assuming UEs has location information from each other.

The change of transmission starting point can be implemented by using a shorter CP extension in comparison to CP extension to be applied by UE B, or by puncturing the start of the AGC symbol which is present in the beginning of the Sidelink slot.

The basic principle of the mechanism is to ensure that, if UE B succeeds to start a transmission on interlace b , then UE A should be automatically blocked to start transmitting on interlace a by the LBT procedure (as the LBT will sense the energy of UE B transmission which starts earlier), therefore the transmission of UE B, if occurring, will not be harmed by the IBE from UE A. And if UE B transmission does not actually start on the reserved resource (e.g., due to LBT failure, re-evaluation, or transmission dropping) or if UE B moves away, then UE A still has a chance to start transmitting on interlace a later.

In another example illustrated in Figure 24-C, a UE A which is preparing to transmit on a selected resource on an interlace a , if it senses a resource reservation from a UE B on an interlace b and the separation in frequency w between the interlaces is within at least one interval $W=[wL, wH]$, UE A may change its

transmission starting point to be earlier than the starting point of the transmission of UE B, based on one or more of the following criteria:

- Resource reservation of UE B is for a transmission of lower priority than of UE A.
- Resource reservation of UE B has an estimated receive power y higher than Y .
- Distance d between receiver of UE A and the transmitter UE B is lower than a value D .

The change of transmission starting point can be implemented applying a longer CP extension in comparison to CP extension applied by UE B.

In this case, the basic principle is that transmission of UE A (e.g. of higher priority) starts earlier and blocks the start of the lower priority transmission of UE B in the adjacent interlace, i.e. avoiding the lower priority transmission to cause IBE issues to the higher priority one at least in the vicinity area.

The main advantage of this solution is that it allows protecting transmissions, e.g. of high priority, from the effect of IBE without changes on scheduling or UE coordination mechanisms, since the blocking of an IBE source transmission from UEs in vicinity relies on the LBT outcome. The downside of this solution is that it increases the dropping rate of low priority transmissions.

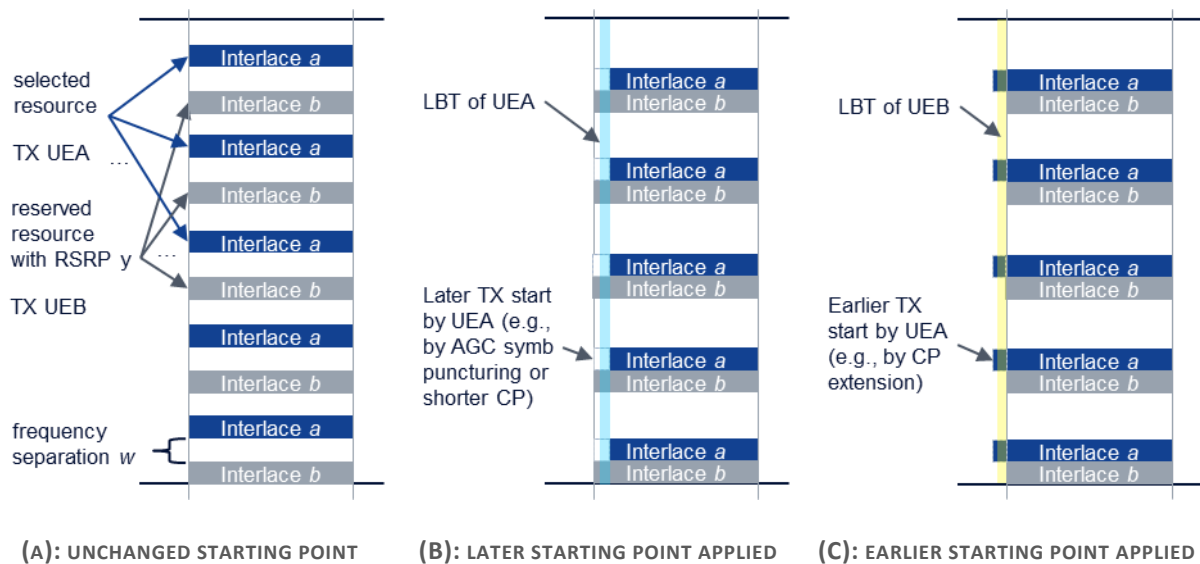


FIGURE 24: EXAMPLE OF CHANGING TRANSMISSION STARTING POINT FOR BLOCKING IBE SOURCE TRANSMISSION

- Enabler D: IBE aware inter-UE coordination mechanisms

In this solution, the subnetwork devices should exchange resource reservation, e.g. through ePDCCH for coordination between HC-HC and sPDCCH for coordination between HC-SNE as mentioned in previous section, and additionally the indication may also include an information of power class or expected transmit power in the reserved resources of the sub-pools. The receiving devices sensing the reservations can then determine how severe the IBE will impact its reception and based on that it provides this information to the transmitting device, such that resources prone to suffer from IBE issues are indicated as non-preferable resources. As shown in Figure 25, the implementation of this solution can be based on enhancing the Sidelink IUC framework such that a UE can determine its preferred/non-preferred resources in IUC scheme 1 considering the impact of IBE from one interlaced RB or contiguous RB sub-channel to another. That includes IBE aware triggers for requesting or sending IUC Scheme 1 indications. The conditions to include a sub-channel in the set of non-preferred resource may follow similar criteria as described in Enabler C.

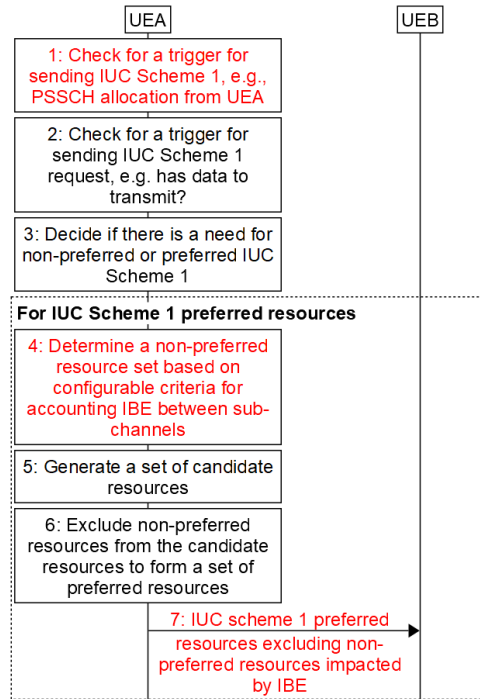


FIGURE 25: IBE-AWARE INTER-UE COORDINATION SCHEME (RED STEPS HIGHLIGHT IMPACT ON EXISTING IUC PROCEDURE).

4.3 NEXT STEPS

In the study presented above, it is assumed that HC-to-HC and SNE-to-HC communication are not multiplexed together in a same band. That already helps avoiding that IBE leakage of high-power communication towards low power communication resources, as well as other issues such as AGC adjustment. However, it implies that enough bandwidth is available to separate the channels of HC-to-HC link from the SNE-to-HC link. In future studies we should consider coexistence of these two types of communication in a shared band. That includes studying the impact on the performance when high and low power subnetworks communication are time-frequency multiplexed in the same band assuming firstly that reservations are not IBE aware, as a baseline. And further, some selected IBE mitigation methods that can be applicable for licensed or unlicensed bands should be studied, such as stricter IBE requirements and the use of semi-static sub-pools reservations assuming the devices are IBE-aware.

5 DETECTION AND MITIGATION OF EXTERNAL INTERFERENCE

Subnetworks may not only suffer from interference coming from other subnetworks, but also from interference created by other radio technologies active in the same location (in case they are operating over the same spectrum), and potential malicious interferers (e.g., jammers). We present here potential solutions for detecting and mitigating such external interferers. The solutions presented here are mainly to be applied to industrial and in-vehicle use cases, where external interference can be a serious threat to the critical applications to be supported.

Networks and smart factories are becoming more agile, flexible, variable, and therefore more complex. This ever-increasing complexity makes it difficult for operators to monitor processes and identify deviations. Problems and failures are often detected too late, and maintenance intervals are not chosen correctly. Intelligent systems for early detection of anomalies or mitigating interference can provide significant relief by detecting deviations at an early stage and avoiding production downtime.

In the following, we present in section 5.1 a brief background on types of anomalies from a general perspective, then section 5.2 shows anomaly detection methods and approaches. These two sections represent a general framework and introduction into radio related techniques used to detect and mitigate cellular and non-cellular interference discussed in the last section 5.3 and will build upon it on future contributions.

5.1 TYPES OF ANOMALIES

The field of anomaly detection tries to identify instances of a dataset that are unusual or differ significantly from most of the data. Anomalies differ decisively in their occurrence, where they can be divided into three types:

Global/point Anomalies

This category represents the simplest outlier type and is the focus of most research papers. A single Global or Point anomaly can be defined as an instance of data that can be classified as anomalous with respect to entire dataset. In Figure 26, in 2D space, a single point shows up, where clearly the dataset can be divided into three clusters. Since the suspected pointed cannot be mapped to any of them, it is classified as anomaly point.

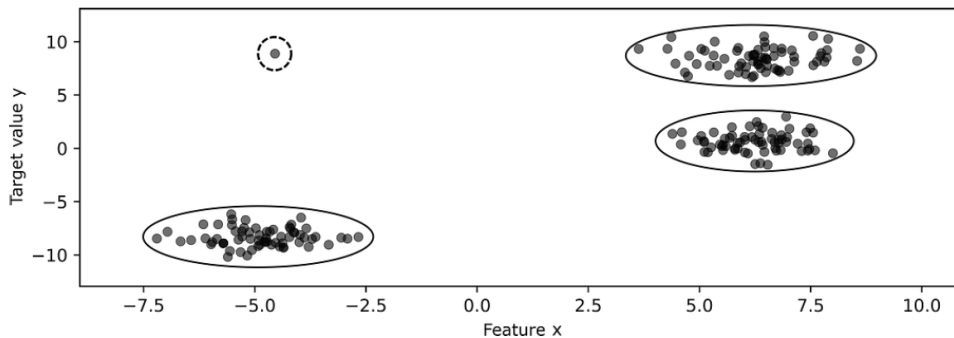


FIGURE 26: POINT ANOMALY EXAMPLE IN A 2D DATASET.

Collective Anomalies

In each dataset, a collective of related instances of anomaly can be identified as anomalous; and so-called collective anomalies. However, by looking at these instances individually, these may not be recognized as an anomaly, but their occurrence in the collective justifies a designation as an outlier when compared to the overall dataset, as shown in the Figure 27.

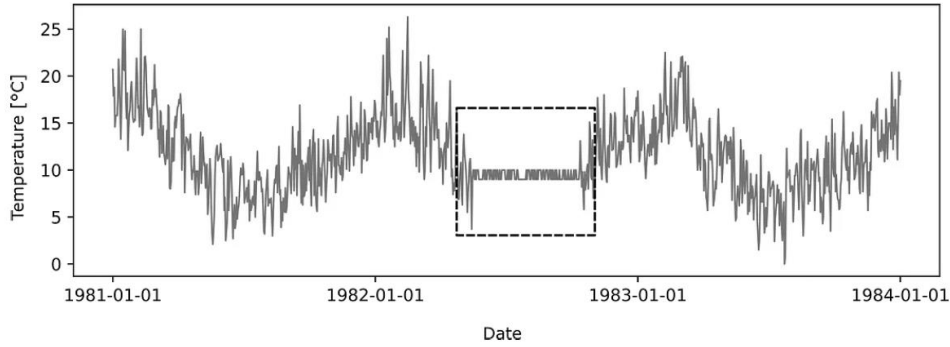


FIGURE 27: COLLECTIVE ANOMALY REPRESENTATION IN AIR TEMPERATURE RECORDS.

Contextual Anomalies

An instance is classified as contextual anomaly if it appears to be anomalous in a specific context. For instance, in the Figure 28, the marked data points represent unusual observed temperatures.

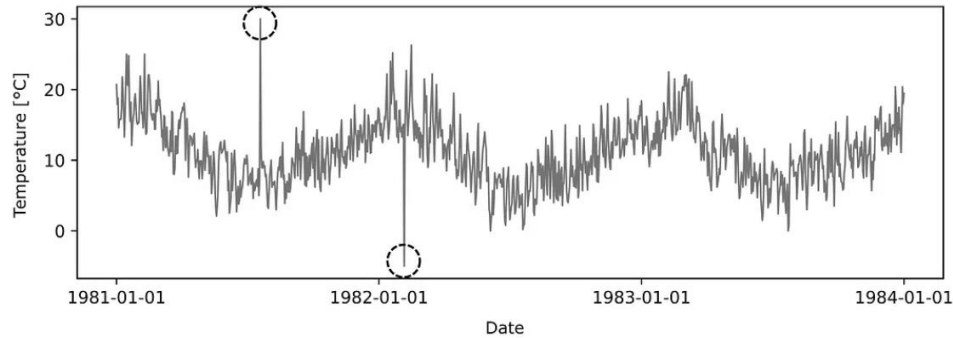


FIGURE 28: CONTEXTUAL ANOMALIES REPRESENTATION IN AIR TEMPERATURE RECORDS

5.2 ANOMALY DETECTION AND CLASSIFICATION METHODS

In the following, different classification methods are listed. Probabilistic methods consider certain probabilistic assumptions about the occurrence of events. The evaluation of instances is considered in terms of their probability distribution. Instances with very low probability are defined as outliers. The robust covariance estimator works according to this principle.

- Distance and Density methods: Non-parametric methods consider and evaluate data points in relation to their environment. If there are enough similar data points around an anchor data point, the data will be classified as normal. This similarity is usually represented by the distance between the data points. The k -nearest neighbour algorithm works on this principle.
- Clustering methods: These methods look for grouping of similar objects and structures. Instances are grouped in such a way that the data within a group is as similar as possible, but the data of different partitions is as different as possible. Instances that cannot be assigned to any group are classified as outliers.
- Reconstruction methods: These methods attempt to detect patterns in the data, with the aim of being able to reconstruct the signal without noise. Well-known algorithms that belong to these are for example, Principal Component Analysis (PCA) and Replicator Neural Networks (RNN).

Most approaches try to model the regions in feature space that describe the normal behaviour of the process under consideration. Anomalous data is defined as data outside the defined region. However, several factors

challenge this relatively simple approach. In practice, it is usually not possible to clearly define the normal region, the boundaries between normal and anomalous behaviour are not always clear. The set of all samples of normal and anomalous behaviour can be described by probability distributions. Both distributions are rarely separated from each other, and an overlap arises, thus a unique classification of normal instances and anomalies is not possible.

Anomaly detection algorithms usually evaluate each data point with an anomaly score, which is a preliminary step for subsequent decision-making. Samples are classified as anomaly or normal with respect to the anomaly score according to a predefined threshold. The threshold value represents system sensitivity and depicts a hyperparameter that needs to be designed for each use case, where an evaluation of the misclassification consequences should be tackled. The True Positive Rate (TPR) and False Positive Rate (FPR) are indispensably a trade-off with each other. For example, decreasing the threshold will result in increasing both TPR and FPR.

Determining the optimal threshold value that leads to the primary expected goal requires additional knowledge about the process. In industry, the cost-optimal threshold is the primary goal especially when considering commercial applications. For instance, an equipment failure and huge repair work can result if an anomaly cannot be detected, while a threshold that results in high FPR leads to a great control effort. For the sake of completeness and to explain this trade-off further, the literature uses a healthcare example. In cancer detection tests, a low threshold is appropriate. Failure to detect the test in a healthy patient merely leads to further testing, whereas failure to detect early-stage disease reduces the patient's likelihood of survival. Thus, a high TPR is weighted higher than a low FPR.

5.2.1 ALGORITHMS AND METHODS USED FOR ANOMALY DETECTION.

In anomaly detection field, a vast variety of different algorithms and approaches are used in the literature. Figure 29 depicts a structure of well-known methods in this field. Two main categories are often used. The first category focuses on unsupervised outlier detection, where robust covariance estimator, Isolation Forest, one class Support Vector Machine (SVM), and autoencoders in the field of deep learning are primarily used. The second category primarily considers model-based approaches like time series analysis and regression analysis. With the help of model-based approaches, models are set up which can reproduce and predict the behaviour of a process under consideration.

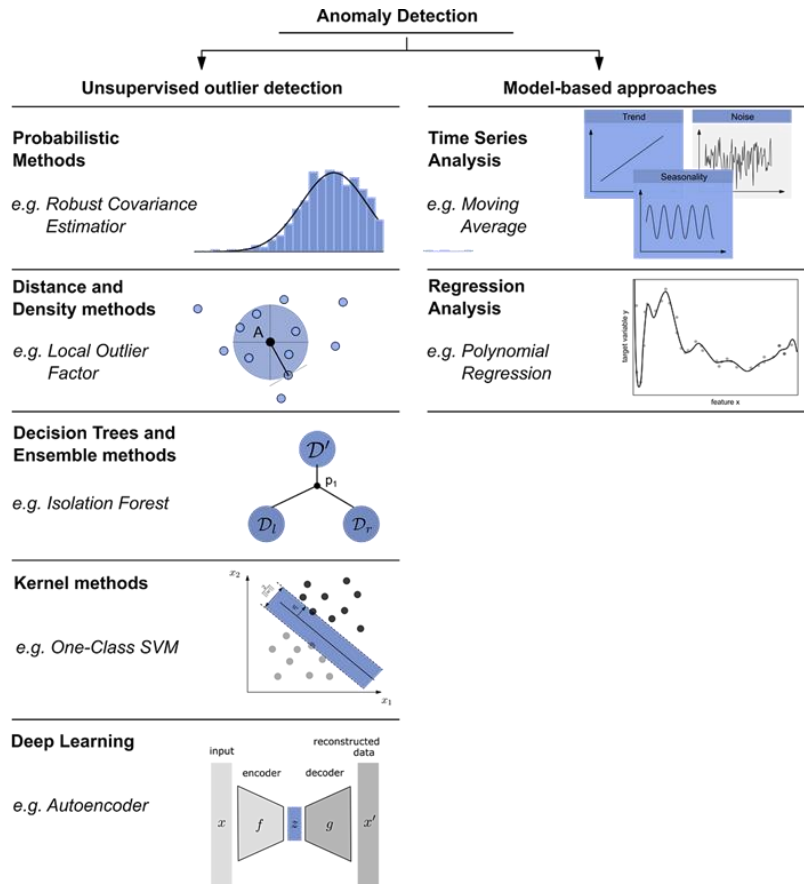


FIGURE 29: AN OVERVIEW OF ANOMALY DETECTION ALGORITHMS

5.3 IN-X-SUBNETWORKS EXTERNAL INTERFERENCE MITIGATION

Interference poses a significant challenge within dense subnetworks, potentially impeding the stringent communication demands related to throughput, latency, and reliability. Consequently, extensive research focuses on interference management and mitigation techniques to address this issue. Besides intra- and inter-cell interference, the system needs to be robust in managing different types of radio interference, that could be caused by rare events while still being very troublesome. Regarding the in-X subnetworks, two important sources of non-cellular forms of interference that need to be considered and represent an important area for future research are: jamming attacks and impulsive noise.

5.3.1 IN-X-SUBNETWORKS CELLULAR AND NON-CELLULAR INTERFERENCE TYPES

The deployment of in-X subnetworks can result in dense scenarios, potentially leading to high interference levels. Common examples include congested roadways with numerous vehicles, or robots in a crowded factory. In certain situations, subnetworks may even coexist in the same physical location. For instance, an in-body subnetwork installed in a person sitting inside a car could share space with an in-vehicle subnetwork. While short-range transmission, extensive spectrum utilization, and spatial/frequency diversity enhance the desired receive signal, external interference remains a critical concern, particularly for life-critical services. A major consequence of in-X subnetworks is heterogeneous systems, and the wide variability of environments leads to potentially impactful interference. Future in-X networks will face two challenges: robustness and adaptability, with high energy and lifetime constraints.

Impulsive noise is an unintentional process that comprises cellular and non-cellular interference. While the non-cellular can be generated by industrial machineries or robot movement, the cellular impulsive noise may arise from a realistic physical mechanism under some reasonable assumptions and conditions. Increasing the number of communication devices without more available frequency bands inevitably implies stricter spatial reuse of radio resources. If we try to limit interference (interference alignment) or to consider them as a signal (Network Coding [30]), high complexity arises because of the required knowledge of timing and channel response. Moreover, trying to create systems without interference is a sub-optimal strategy [31]. Alternatively, the optimal approach is to consider the interference as noise and create codes that take advantage of it [31]. However, if they are considered as noise, their statistical nature depends strongly on the environment, and they are often not Gaussian but have impulsive characteristics [32]. The problem is that most of the communication systems implemented are based on Gaussian assumption: the capacity is well studied with additive Gaussian noise, but less with impulsive interference; the conventional linear receiver under the Gaussian noise assumption is not suited anymore and new strategies must be implemented; even the SNR is not sufficient to represent the link quality and another criterion must be defined.

Intended malicious smart jammers can disrupt the communication link quality and pose a major threat to meeting extreme performance requirements. A smart jammer can indeed learn timing, frame, and traffic pattern of an in-X subnetwork, with periodic traffic that characterizes most of the control loops and emulate its transmissions with potentially disruptive effects. When jamming occurs, it disrupts communication and can cause performance issues and instability in wireless networked control systems.

Even if jamming seems a more dangerous threat because it is caused by a malicious attacker, whereas the impulsive noise is an unintentional process as described previously, the system still needs to be robust against both cellular and non-cellular forms of interference; even if they might be considered as rare events in the existing systems. These types of interference are very troublesome to the system performance, especially when we consider life-critical services .

5.3.2 PHYSICAL MECHANISMS THAT LEAD TO NON-CELLULAR INTERFERENCE.

Network heterogeneity comes out in ad-hoc networks and small-cells due to the variations in transmit power constraints and the varied placement of the transmitters. In-X subnetworks satisfy these characteristics, thus are considered as heterogenous networks. In heterogenous networks like in-X subnetworks, different transmission protocols in a common band are used, and multiple applications are considered, etc, resulting in different data types and different symbol durations as shown in Figure 30. Physical mechanisms that lead to noise which is impulsive by nature and characterized by heavy-tailed distributions may be generated by the following conditions.

- Multiple coexisting communication systems that share the same band, for instance, the ISM band.
- The rapid change in time of the active set of transmitting devices (e.g., machine-to-machine communications, where rare and short packets are transmitted).
- Uncoordinated access between different networks, such as Sigfox and LoRa (using ALOHA).
- Different PHY and MAC layer protocols.
- Different data types.
- Different symbol durations.
- Different data traffic flows.

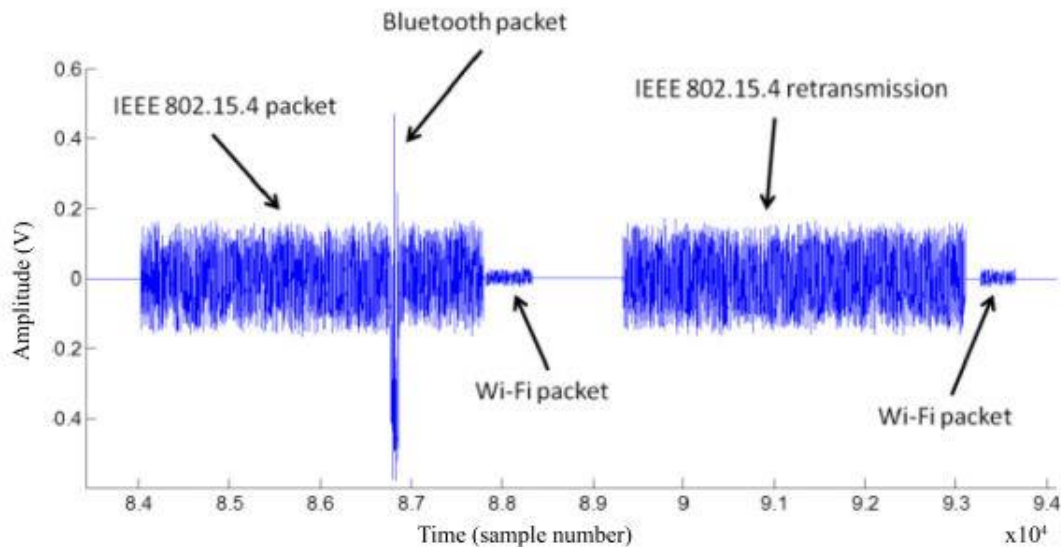


FIGURE 30: COEXISTENCE OF TECHNOLOGIES IN THE 2.4-GHZ BAND. MEASUREMENTS MADE BY THE NATIONAL INSTRUMENTS USRP [33]

5.3.3 NON-CELLULAR INTERFERENCE DISTRIBUTIONS

Some classical noise models encountered in the literature are reviewed in this sub-section. The Gaussian noise model represents accurately the thermal noise in the receiver. However, dealing with dense and heterogeneous networks, i.e. future networks, the interference may exhibit impulsive behaviours [32] and the Gaussian assumption is no longer suited. Thus, several approaches have been discussed in [34] to consider the impulsive behaviour that includes:

- Theoretical approaches (e.g., alpha-stable distributions, Middleton class A distributions, etc.).
- Mixture model approach (e.g., Gaussian mixture, Generalized Gaussian mixture, epsilon-contaminated, etc.).
- Empirical approaches (e.g., Pareto model, T-student model, etc.).

One can note that the models cover the main solutions and are not an extensive list of the different impulsive models. Furthermore, the extreme reliability requirements of life-critical applications supported by the in-X subnetworks require a detailed characterization of the tail of the interference distribution; accordingly, these approaches consider heavy tailed distributions instead of exponential distributions that captures well the characteristics of the Gaussian noise.

Main challenges to consider when dealing with heavy tailed distributions:

- Statistical moments: Almost do not exist.
- PDF for most distributions: no closed expression.
- Conventional receivers are designed based on Gaussian assumption.
- Adopting heavy tailed distribution for receiver design: Receivers become complex and computationally prohibitive.
- Dynamic interference at different realizations as shown in Figure 31 (top), where six different examples of interference realizations from different models are represented.
- Detection: Non-linear decision regions as shown in Figure 31 (bottom), where the decision regions that the optimal receiver must produce in a binary case under different interference models.

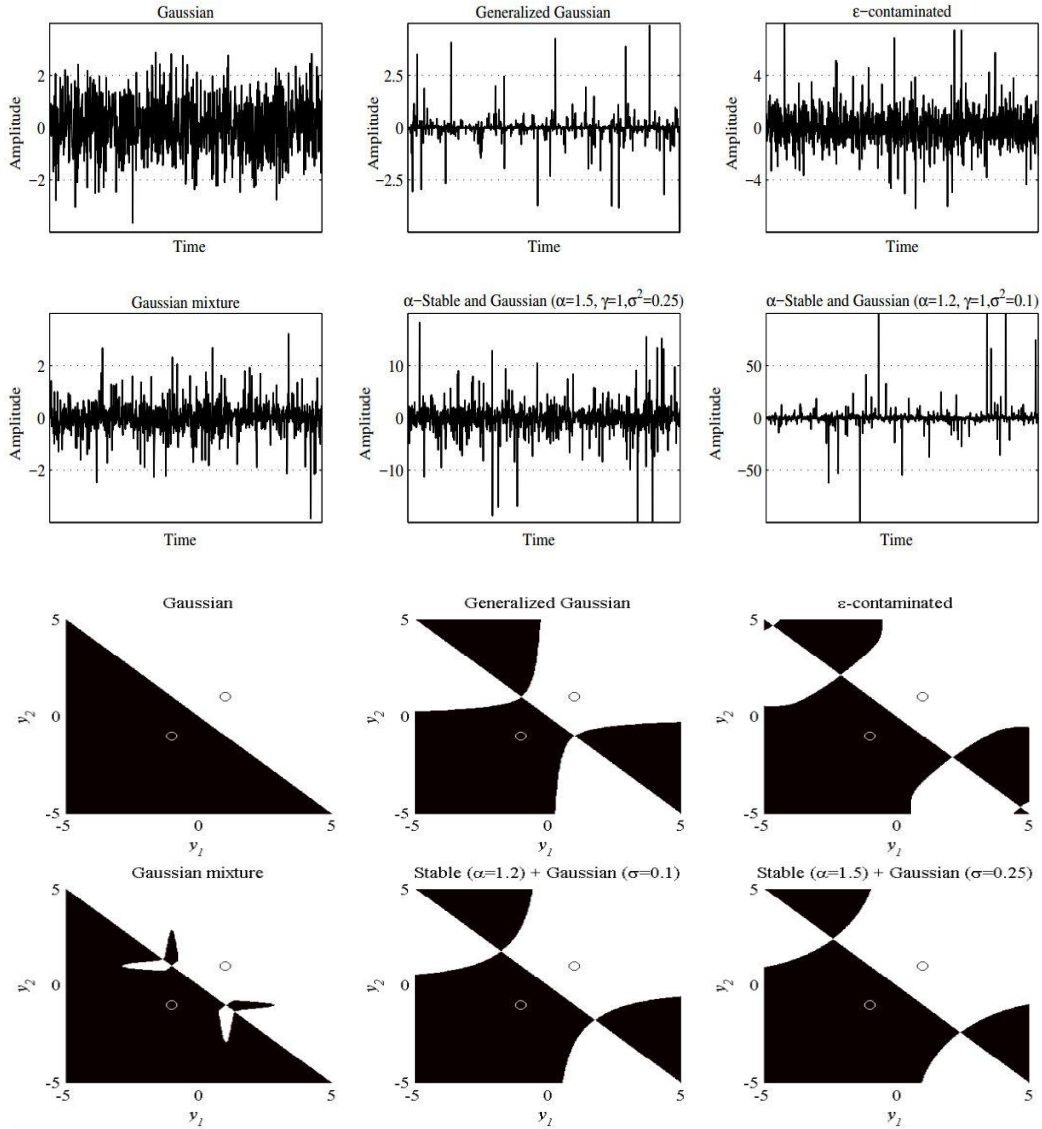


FIGURE 31: (TOP) EXAMPLE REALIZATIONS FOR EACH DIFFERENT SUB-EXPONENTIAL IMPULSIVE NOISE PROCESSES. (BOTTOM) OPTIMAL DECISION REGIONS FOR THE DIFFERENT INTERFERENCE PROCESSES [34].

In the literature, different channels models are represented for the impulsive noise. However, alpha-stable distributions shows a big interest for different reasons starting from theoretical proofs as shown in [32][34], to the Generalized Central Limit Theorem (GCLT) which states that the only possible non-trivial limit of normalized sums of i.i.d terms (without finite variance) is stable also for some experimental measurements that match with stable distributions [32].

TABLE 7: PARAMETER DESCRIPTION OF STABLE DISTRIBUTION

Parameter	Name	Range
α	characteristic exponent	$(0,2]$
$\beta = 0$	skew parameter	$[-1, +1]$
γ	scale parameter	$(0, +\infty)$
$\delta = 0$	location parameter	$(-\infty, +\infty)$

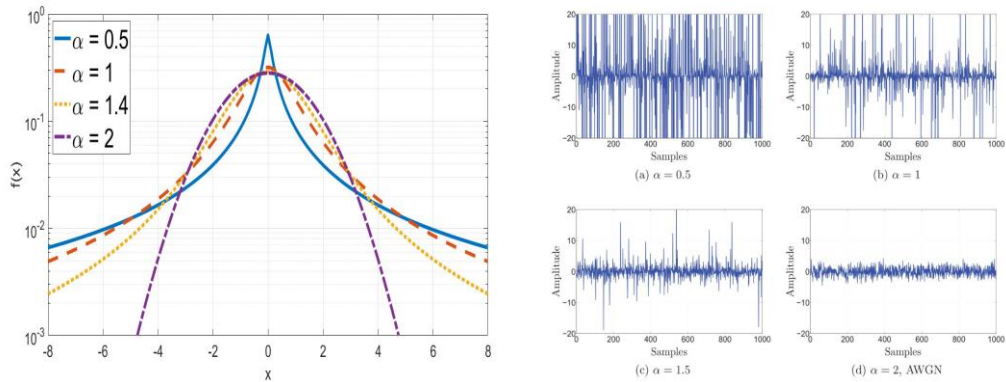


FIGURE 32: EFFECT OF THE CHARACTERISTIC EXPONENT PARAMETER α ON THE α -STABLE PDF

Table 8 represents the different parameters of alpha-stable distributions, along with the range for each parameter. The scale parameter gamma is alternative to the noise variance, alpha represents the heaviness of the tail, beta controls the skewness, and finally, the location parameter is alternative to the mean value. Figure 32 (left) illustrates the effect of the characteristic exponent parameter α on the α -stable PDF, the y-axis is given in a logarithmic scale to highlight the heaviness of the tails for each α . Obviously, as α decreases the tail becomes heavier which delineates a higher probability to receive samples far from the origin. Moreover, for the special case $\alpha = 2$ the tail decreases exponentially and that represent the Gaussian case. Furthermore, in Figure 32 (right), 1000 samples are generated for each distribution considered, showing the impulsiveness behaviours as α decreases and the special case of when $\alpha = 2$ representing the Gaussian noise.

5.3.4 MISMATCH DECODING PROBLEM

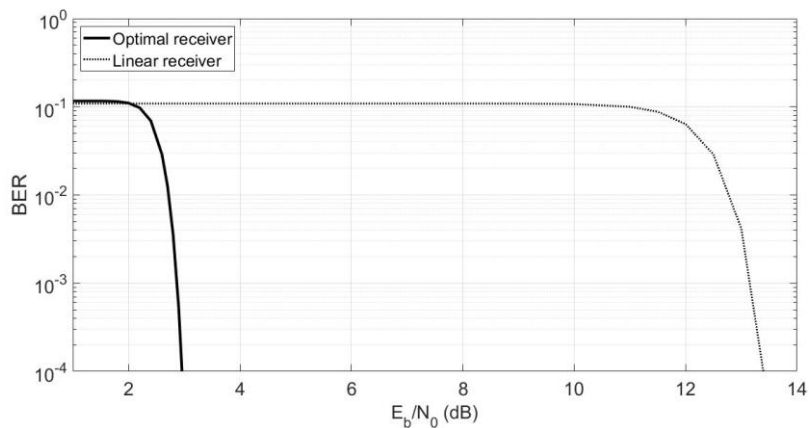


FIGURE 33: EFFECT OF MISMATCH DECODING, WHERE THE LINEAR RECEIVER IS USED IN AN IMPULSIVE ENVIRONMENT.

Regarding the receiver design in the impulsive case, several observations can be noted. Firstly, the significant performance degradation obtained by the linear receiver (optimal for Gaussian noise and simple to implement) is due to the model mismatch as shown in the above Figure 33. Second, the construction of an optimal receiver, which assumes to have knowledge of the channel is complicated as various models can be considered for receiver design, and is difficult to know which one can be robust against environment changes. In addition, if theoretical

impulsive models are considered, it is difficult to implement the receiver. Moreover, if empirical models are chosen to offer analytical solutions, their ability to adapt to different contexts are to be proven.

5.3.5 INTERFERENCE MITIGATION AND RECEIVER DESIGN

Establishing reliable and efficient communications require to consider the impulsive nature while designing the receivers. The interference modelling exhibits in many situations an impulsive behaviour that can be designed by several approaches and different distributions. However, designing a specific receiver for each situation is not efficient as the interference characteristics can highly vary in time and space. Thus, having a receiver able to cope with a large set of different interference models (impulsive or not) and with different degrees of impulsiveness is highly desired.

In the following, without being exhaustive, the different receiver design approaches can be classified into four categories.

- **Optimal approach:** in Gaussian case this is very attractive because it leads to a linear receiver, straightforward to implement. However, with impulsive noise, the log-likelihood ratio (LLR) becomes a non-linear function. Its implementation is complex and highly depends on the noise distribution either because of the lack of a closed-form expression such as for α -stable noise, or because it needs high computational burden such as for Middleton noise. Consequently, the extraction of a simple metric based on the noise PDF in the decoding algorithm is prevented. It is worth mentioning that under the α -stable assumption the LLR can still be computed numerically, for instance, by numerical integration of the inverse Fourier transform of the characteristic function.
- **Noise distribution approximation:** The main idea behind this approach is to find a distribution that well approximates the true noise plus interference PDF, with analytical expression and parameters that can be estimated in a simple manner.
- **Different metric measures:** An alternative way to interpret detection is to consider that the likelihood measures the distance between all the received signals and the possible transmitted signals (e.g., Hubber metric [35], p-norm).
- **Direct LLR approximation:** The LLR for the Gaussian noise is expressed by a linear approximation as a function of the received symbols ($LLR = 2y/\sigma^2$, where y is the received symbol and σ^2 represent the noise variance). Using only a linear scaling whose slope depends on the additive noise variance leads to severe performance loss as soon as noise is impulsive (e.g., due to non-cellular interference types). This performance loss occurs because with this linear scaling, large values in Y result into large LLR. However, under impulsive noise, large values in Y are more likely due to an impulsive event (meaning a less reliable sample) so that the LLR should be smaller. Consequently, a non-linear LLR approximation will be observed, the computation of such non-linear LLR is prohibitive due to the lack of density function in a closed form.

So, we consider parametric approximation L_θ of the LLR. The family of functions L_θ is chosen for its simplicity and flexibility to represent the LLR in different channel types. To narrow down the search, we consider the estimated LLR L_θ is an odd piece-wise function. In particular, we consider both demappers L_{ab} and L_{abc} [36] as shown in Figure 34, that outperforms other LLR approximations as shown in [37], in terms of performance.

$$L_{ab}(y) = \text{sgn}(y) \min(a|y|, b/|y|) = \begin{cases} ay & \text{if } |y| < \sqrt{b/a}, \\ b/y & \text{otherwise,} \end{cases}$$

$$L_{abc}(y) = \text{sgn}(y) \min(a|y|, b/|y|, c) = \begin{cases} ay & \text{if } |y| < c/a, \\ c & \text{if } c/a < |y| < bc, \\ b/y & \text{if } |y| > bc. \end{cases}$$

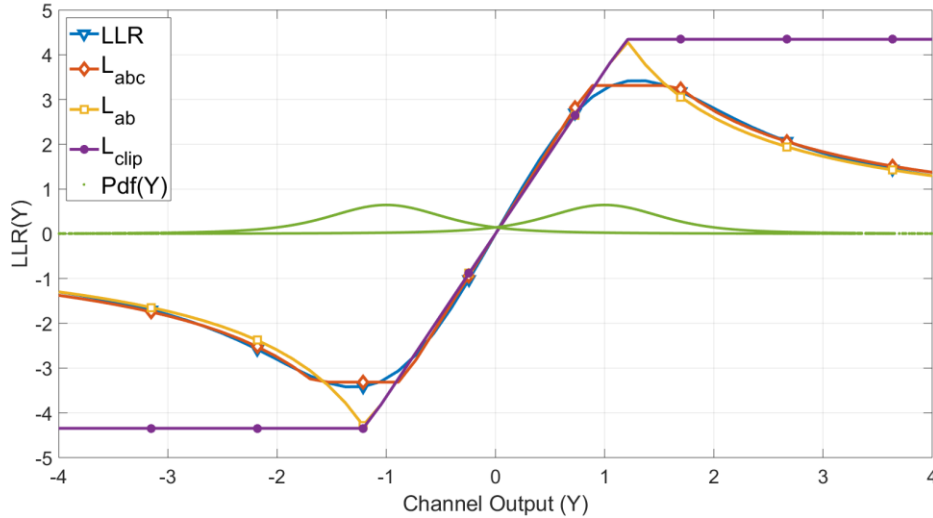


FIGURE 34: COMPARISON OF THE OPTIMAL LLR SHAPE WITH DIFFERENT APPROXIMATIONS.

The LLR approximations depend on several parameters, which must be optimized to make the approximation as close as possible to the LLR. Several parameter estimation methods are considered in the literature. In [38], the authors proposed a framework to enable online real-time parameter estimation, but they consider long block length regime. For short packets as in in-X Subnetworks the proposed framework suffers from significant performance degradation due to the lack of availability of large number of samples. To solve this problem, authors in [39] proposed a solution that enables unsupervised learning in the short block length regime which is suitable for in-X Subnetworks.

In order to show the robustness of the proposed framework, authors in [32] investigated the performance in terms of BER simulations in different channel types, e.g., Gaussian and non-Gaussian (stable, Middleton, contaminated, Gaussian-mixture, etc.) and with different impulsive states (e.g., low, modern, high impulsive). The approximation family has to be wide enough to encompass the linear behaviour of exponential-tail noises like the Gaussian and the non-linear behaviour of sub-exponential distributions of the impulsive noises. The estimation of the LLR approximation parameter relies on an information theory criterion that do not depend on any noise assumption. In [32] results show that the receiver design is efficient in a large variety of noises and that the supervised and unsupervised estimation allows to reach performance close to the optimal approach. Furthermore, the unsupervised estimation benefit from the whole received sequence to increase the useful data rate.

5.3.6 NEXT STEPS AND PERSPECTIVES

One main problem behind this proposal is that the framework needs to be extended to encompass higher order modulations, where such modulations will have different LLR patterns that may require different LLR approximation functions. In addition, the estimation complexity of the parameters can still be reduced to match low computational unit capabilities that may arise in the in-X subnetworks. We aim in the future to tackle these problems using different Anomaly detection candidates discussed in section 5.1 and 5.2 (e.g., autoencoders), in order to have a universal framework that can be extended to a wider range of channel types and higher order

modulations without suffering from mismatch problems or approximation degradations as illustrated in the Figure 35. In brief we would like to find ubiquitous framework using AIML methods to cover

- Wider range of LLR approximation functions.
- Wider range of distributions.
- Cover Higher-order Modulations.

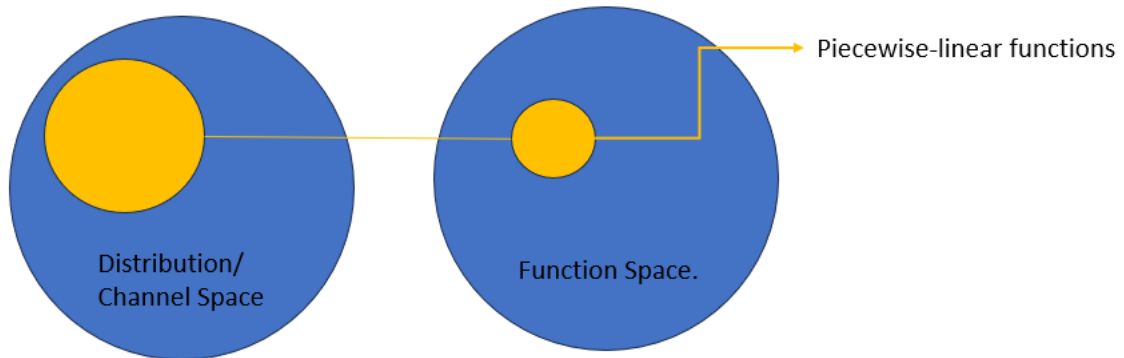


FIGURE 35: MAPPING BETWEEN DISTRIBUTION SPACE AND LLR APPROXIMATION FUNCTIONS SPACE.

6 CONCLUSIONS

This deliverable presented an initial description of innovative strategies for optimizing RRM within the realm of 6G in-X subnetworks, including some preliminary results. It explored various RRM strategies tailored for distinct scenarios, from centralized to distributed and hybrid approaches, highlighting their potential to substantially enhance spectral efficiency and service reliability. Notably, the application of machine learning algorithms provided a robust solution for addressing RRM complexities, such as fluctuating channel conditions and pervasive interference. For instance, in a factory scenario with dense subnetworks installed in robots or production modules, the introduced DNN-based sub-band allocation method effectively met the diverse rate requirements of subnetworks, improving the likelihood of achieving required rates by 20% compared to existing benchmarks. In scenarios where some subnetworks lack access to the centralized controller, it has been demonstrated that even simple approaches, such as a combination of centralized and distributed methods like SISA and Greedy, can significantly enhance performance compared to when disconnected subnetworks randomly select a sub-band.

The exploration of advanced methodologies for distributed power control, particularly through GNNs and MPNNs, has been proposed, focused on adaptability to dynamic network changes, including the addition of new subnetworks. The Air-MPNN framework can reduce signaling overhead with over-the-air aggregation mechanisms, potentially enabling applications requiring ultra-reliable low-latency.

The goal-oriented RRM framework can mark a significant progression in merging communication and control operations. This approach not only enhances traditional network metrics like SINR but also integrates control system KPIs, such as AGV mission times, balancing control applications and network efficiency. Reinforcement learning is identified as a promising approach for such goal-oriented design.

The pivotal role of advanced RRM enablers in enhancing communication within and between subnetworks particularly in a 3GPP context was discussed. Innovations such as the evolution of NR Sidelink provide critical support for integration with future 6G networks and facilitated effective communication strategies, from device-to-device interactions to communication with the parent network. These advancements are crucial for ensuring robust intra-subnetwork communication and efficient coordination across subnetworks. A mechanism for subnetwork resource pool reservation has been proposed. The substantial impact of In-Band Emissions (IBE), particularly in scenarios involving frequency domain multiplexing of subnetwork traffic, was demonstrated. For instance, we noted significant differences in the 50th percentile values for interlaced and contiguous sub-band allocation, showing differences of 30.8 dB and 19.6 dB, respectively, compared to baseline idealistic cases where the IBE effect is not considered, especially under high load scenarios. Potential enablers to address these challenges were also proposed.

Additionally, it has been discussed that the detection and mitigation of external interference are critical for sustaining robust communication systems, especially in environments where multiple radio technologies and potential malicious threats, such as jammers, coexist.

Future research will aim to refine and evaluate these strategies and develop adaptive RRM frameworks capable of responding dynamically to changes in the subnetwork environment and user demands. This task seeks to establish a resilient, efficient, and scalable RRM infrastructure to meet the growing demands of next-generation wireless systems, ensuring robust, high-quality communication in the 6G era. Final results will be presented in deliverable D4.3, and benchmarked against the performance targets defined in the proposal.

REFERENCES

- [1] M. Series, "IMT Vision—Framework and overall objectives of the future development of IMT for 2020 and beyond," *Recomm. ITU*, vol. 2083, no. 0, 2015.
- [2] 6G-SHINE Deliverable D2.2 "Refined definition of scenarios use cases and service requirements for in-X subnetworks", submitted in February 2024.
- [3] D. Li, S. R. Khosravirad, T. Tao, and P. Baracca, "Advanced frequency resource allocation for industrial wireless control in 6G subnetworks," in *2023 IEEE Wireless Communications and Networking Conference (WCNC)*, IEEE, 2023, pp. 1–6.
- [4] S. Bagherinejad, T. Jacobsen, N. K. Pratas, and R. O. Adeogun, "Comparative Analysis of Sub-band Allocation Algorithms in In-body Sub-networks Supporting XR Applications." *arXiv*, Mar. 18, 2024.
- [5] D. Abode, R. Adeogun, and G. Berardinelli, "Power Control for 6G Industrial Wireless Subnetworks: A Graph Neural Network Approach," in *2023 IEEE Wireless Communications and Networking Conference (WCNC)*, IEEE, 2023, pp. 1–6.
- [6] H. Sun, X. Chen, Q. Shi, M. Hong, X. Fu, and N. D. Sidiropoulos, "Learning to optimize: Training deep neural networks for interference management," *IEEE Trans. Signal Process.*, vol. 66, no. 20, pp. 5438–5453, 2018.
- [7] R. Adeogun, "Unsupervised Deep Unfolded PGD for Transmit Power Allocation in Wireless Systems," in *2023 IEEE 34th Annual International Symposium on Personal, Indoor and Mobile Radio Communications (PIMRC)*, IEEE, 2023, pp. 1–5.
- [8] D. Abode, R. Adeogun, L. Salaün, R. Abreu, T. Jacobsen, and G. Berardinelli, "Unsupervised Graph-based Learning Method for Sub-band Allocation in 6G Subnetworks." *arXiv preprint arXiv:2401.00950*, Dec. 13, 2023.
- [9] L. Zdeborová, and F. Krzakała. "Phase transitions in the coloring of random graphs." *Physical Review E* 76, no. 3 (2007): 031131.
- [10] 3GPP TR 38.901, "5G; Study on channel model for frequencies from 0.5 to 100 GHz." v17.1.0.
- [11] S. Lu, J. May, and R. J. Haines, "Effects of correlated shadowing modeling on performance evaluation of wireless sensor networks," in *2015 IEEE 82nd Vehicular Technology Conference (VTC2015-Fall)*, IEEE, 2015, pp. 1–5.
- [12] S. Hakimi, R. Adeogun, G. Berardinelli, "Rate-conforming Sub-band Allocation for In-factory Subnetworks: A Deep Neural Network Approach," [*Status: Accepted at EuCNC 2024*].
- [13] Y. Gu, C. She, Z. Quan, C. Qiu, and X. Xu, "Graph neural networks for distributed power allocation in wireless networks: Aggregation over-the-air," *IEEE Trans. Wirel. Commun.*, 2023.
- [14] A. Mahmood, M. I. Ashraf, M. Gidlund, and J. Torsner, "Over-the-air time synchronization for URLLC: Requirements, challenges and possible enablers," in *2018 15th International Symposium on Wireless Communication Systems (ISWCS)*, IEEE, 2018, pp. 1–6.
- [15] M. Aizat, N. Qistina, and W. Rahiman, "A Comprehensive Review of Recent Advances in Automated Guided Vehicle Technologies: Dynamic Obstacle Avoidance in Complex Environment Toward Autonomous Capability," *IEEE Trans. Instrum. Meas.*, vol. 73, pp. 1–25, 2024, doi: 10.1109/TIM.2023.3338722.
- [16] D. Yang, C. Su, H. Wu, X. Xu, and X. Zhao, "Construction of Novel Self-Adaptive Dynamic Window Approach Combined With Fuzzy Neural Network in Complex Dynamic Environments," *IEEE Access*, vol. 10, pp. 104375–104383, 2022, doi: 10.1109/ACCESS.2022.3210251.
- [17] B. Akgun *et al.*, "Interference-Aware Intelligent Scheduling for Virtualized Private 5G Networks," *IEEE Access*, vol. 12, pp. 7987–8003, 2024, doi: 10.1109/ACCESS.2024.3350513.

- [18] L. M. Amorosa *et al.*, “An End-To-End Analysis of Deep Learning-Based Remaining Useful Life Algorithms for Safety-Critical 5G-Enabled IIoT Networks,” in *2023 IEEE 34th Annual International Symposium on Personal, Indoor and Mobile Radio Communications (PIMRC)*, Sep. 2023, pp. 1–6. doi: 10.1109/PIMRC56721.2023.10293815.
- [19] H. Vietz, A. Löcklin, H. Ben Haj Ammar, and M. Weyrich, “Deep learning-based 5G indoor positioning in a manufacturing environment,” in *2022 IEEE 27th International Conference on Emerging Technologies and Factory Automation (ETFA)*, Sep. 2022, pp. 1–4. doi: 10.1109/ETFA52439.2022.9921635.
- [20] T. Tanagi and K. Adachi, “Dynamic Path Planning for QoS Improvement in Multiple Automated Guided Vehicles,” in *2023 VTS Asia Pacific Wireless Communications Symposium (APWCS)*, Aug. 2023, pp. 1–5. doi: 10.1109/APWCS60142.2023.10234027.
- [21] R. Bejarano, U. D. Atmojo, J. O. Blech, and V. Vyatkin, “Towards enhanced live visualization based on communication delay prediction for remote AGV operation,” in *2021 26th IEEE International Conference on Emerging Technologies and Factory Automation (ETFA)*, Sep. 2021, pp. 01–04. doi: 10.1109/ETFA45728.2021.9613513.
- [22] P. M. de Sant Ana, N. Marchenko, P. Popovski, and B. Soret, “Age of loop for wireless networked control systems optimization,” in *2021 IEEE 32nd Annual International Symposium on Personal, Indoor and Mobile Radio Communications (PIMRC)*, IEEE, 2021, pp. 1–7.
- [23] P. M. de Sant Ana, N. Marchenko, B. Soret, and P. Popovski, “Goal-Oriented Wireless Communication for a Remotely Controlled Autonomous Guided Vehicle,” *IEEE Wirel. Commun. Lett.*, vol. 12, no. 4, pp. 605–609, Apr. 2023, doi: 10.1109/LWC.2023.3235759.
- [24] R. S. Sutton and A. G. Barto, *Reinforcement learning: An introduction*. MIT press, 2018.
- [25] 3GPP TS 38.300, “NR; NR and NG-RAN Overall description; Stage-2.” v18.0.0.
- [26] 3GPP TS 38.214, “5G; NR; Physical layer procedures for data.” clause 8.1.
- [27] D. Li and Y. Liu, “In-Band Emission in LTE-A D2D: Impact and Addressing Schemes,” in *2015 IEEE 81st Vehicular Technology Conference (VTC Spring)*, May 2015, pp. 1–5. doi: 10.1109/VTCspring.2015.7145876.
- [28] 3GPP TS 38.101-1, “NR; User Equipment (UE) radio transmission and reception; Part 1: Range 1 Standalone.” v18.4.0.
- [29] 3GPP TSG RAN WG1, “Final Report of 3GPP TSG RAN WG1 #110 v1.0.0, August 2022.”
- [30] R. Bassoli, H. Marques, J. Rodriguez, K. W. Shum, and R. Tafazolli, “Network Coding Theory: A Survey,” *IEEE Commun. Surv. Tutor.*, vol. 15, no. 4, pp. 1950–1978, 2013, doi: 10.1109/SURV.2013.013013.00104.
- [31] M. Costa, “Writing on dirty paper (Corresp.),” *IEEE Trans. Inf. Theory*, vol. 29, no. 3, pp. 439–441, May 1983, doi: 10.1109/TIT.1983.1056659.
- [32] P. C. Pinto and M. Z. Win, “Communication in a Poisson Field of Interferers—Part I: Interference Distribution and Error Probability,” *IEEE Trans. Wirel. Commun.*, vol. 9, no. 7, pp. 2176–2186, Jul. 2010, doi: 10.1109/TWC.2010.07.060438.
- [33] R. J. Igual Pérez, “Platform Hardware/Software for the energy optimization in a node of wireless sensor networks,” PhD Thesis, Lille 1, 2016.
- [34] Y. Mestrah, “Robust communication systems in unknown environments,” PhD Thesis, Université de Reims Champagne-Ardenne, 2019.
- [35] T. C. Chuah, “Robust iterative decoding of turbo codes in heavy-tailed noise,” *IEE Proc.-Commun.*, vol. 152, no. 1, pp. 29–38, 2005.
- [36] Y. Mestrah, A. Savard, A. Goupil, G. Gelle, and L. Clavier, “Robust and simple log-likelihood approximation for receiver design,” in *2019 IEEE Wireless Communications and Networking Conference (WCNC)*, IEEE, 2019, pp. 1–6.

- [37] Y. Mestrah, A. Savard, A. Goupil, G. Gellé, and L. Clavier, “Mesure indirecte des performances de LLR approché,” in *Proceedings of GretsI*, 2019.
- [38] Y. Mestrah, A. Savard, A. Goupil, G. Gellé, and L. Clavier, “An Unsupervised LLR Estimation with unknown Noise Distribution,” *EURASIP J. Wirel. Commun. Netw.*, vol. 2020, no. 1, p. 26, Dec. 2020, doi: 10.1186/s13638-019-1608-9.
- [39] Y. Mestrah *et al.*, “Unsupervised Log-Likelihood Ratio Estimation for Short Packets in Impulsive Noise,” in *2022 IEEE Wireless Communications and Networking Conference (WCNC)*, Apr. 2022, pp. 944–949. doi: 10.1109/WCNC51071.2022.9771897.